NAVAL POSTGRADUATE SCHOOL

Monterey, California

THESIS

STUDY OF EXPLOSIVE AND NONEXPLOSIVE

CYCLOGENESIS DURING FGGE

by

Eric J. Wright

December 1988

Thesis Advisor: C. H. Wash

Unclassified

security classification of this page

REPORT DOCUMENTATION PAGE

1a Report Security Classification Unclassified			1b Restrictive Markings
2a Security Classification Authority			3 Distribution Availability of Report: Approved for public release; distribution is unlimited.
2b Declassification Downgrading Schedule			
4 Performing Organization Report Number(s)			5 Monitoring Organization Report Number(s)
6a Name of Performing Organization: Naval Postgraduate School	6b Office Symbol (if applicable): 63		7a Name of Monitoring Organization: Naval Postgraduate School
6c Address (city, state, and ZIP code): Monterey, CA 93943-5000			7b Address (city, state, and ZIP code): Monterey, CA 93943-5000
8a Name of Funding Sponsoring Organization	8b Office Symbol (if applicable)		9 Procurement Instrument Identification Number
8c Address (city, state, and ZIP code)			10 Source of Funding Numbers: Program Element No / Project No / Task No / Work Unit Accession No

11 Title (include security classification): STUDY OF EXPLOSIVE AND NONEXPLOSIVE CYCLOGENESIS DURING FGGE

12 Personal Author(s): Eric J. Wright

13a Type of Report	13b Time Covered	14 Date of Report (year, month, day)	15 Page Count
Master's Thesis	From To	December 1988	87

16 Supplementary Notation: The views expressed in this thesis are those of the author and do not reflect the official policy or position of the Department of Defense or the U.S. Government.

17 Cosati Codes			18 Subject Terms (continue on reverse if necessary and identify by block number)
Field	Group	Subgroup	Cyclogenesis.

19 Abstract (continue on reverse if necessary and identify by block number)

The purpose of this thesis is to analyze and evaluate explosive cyclogenesis during the winter of the First Global GARP Experiment (January to February 1979). Explosive cyclogenesis is defined as a decrease in the sea-level pressure at the rate of one mb per hour for a period of 12 h up to 24 h. The European Centre for Medium-range Weather Forecasts (ECMWF) provided the revised analyses for evaluation and comparison of important cyclone properties in a sample of 13 explosive developing cases and eight nonexplosive cases.

The specific parameters being examined include the static stability, low-level absolute vorticity, vorticity advection, eddy and mean modes of the vorticity transport, upper-level divergence, kinematic vertical velocities and the strength of the low-level baroclinity. These parameters are compared at the initial, 12 and 24 hour time periods as well as the overall 24 hour average. The statistical relationships and magnitudes of these terms indicate the most significant physical mechanisms in explosive cyclone development compared to the nonexplosive storm group.

The important outcome of these results is that the kinematic vertical velocity and the upper-level forcing mechanisms are statistically separable. The large values for the upper-level processes suggest that the upper tropospheric wave influence is most likely producing the stronger vertical motions.

20 Distribution Availability of Abstract	21 Abstract Security Classification	
☒ unclassified unlimited ☐ same as report ☐ DTIC users	Unclassified	
22a Name of Responsible Individual: Carlyle H. Wash	22b Telephone (include Area code): (408) 646-2295	22c Office Symbol: 63 Wx

DD FORM 1473,84 MAR 83 APR edition may be used until exhausted
All other editions are obsolete

security classification of this page

Unclassified

Approved for public release; distribution is unlimited.

Study of Explosive and Nonexplosive Cyclogenesis during FGGE

by

Eric J. Wright
Lieutenant Commander, United States Navy
B.S., U.S. Naval Academy, 1977

Submitted in partial fulfillment of the
requirements for the degree of

MASTER OF SCIENCE IN METEOROLOGY AND OCEANOGRAPHY

from the

NAVAL POSTGRADUATE SCHOOL
December 1988

Author: Eric J. Wright
Eric J. Wright

Approved by:
Carlyle H. Wash, Thesis Advisor

Russell L. Elsberry, Second Reader

Robert J. Renard, Chairman,
Department of Meteorology

Gordon E. Schacher,
Dean of Science and Engineering

ABSTRACT

The purpose of this thesis is to analyze and evaluate explosive cyclogenesis during the winter of the First Global GARP Experiment (January to February 1979). Explosive cyclogenesis is defined as a decrease in the sea-level pressure at the rate of one mb per hour for a period of 12 h up to 24 h. The European Centre for Medium-range Weather Forecasts (ECMWF) provided the revised analyses for evaluation and comparison of important cyclone properties in a sample of 13 explosive developing cases and eight nonexplosive cases.

The specific parameters being examined include the static stability, low-level absolute vorticity, vorticity advection, eddy and mean modes of the vorticity transport, upper-level divergence, kinematic vertical velocities and the strength of the low-level baroclinity. These parameters are compared at the initial, 12 and 24 hour time periods as well as the overall 24 hour average. The statistical relationships and magnitudes of these terms indicate the most significant physical mechanisms in explosive cyclone development compared to the nonexplosive storm group.

The important outcome of these results is that the kinematic vertical velocity and the upper-level forcing mechanisms are statistically separable. The large values for the upper-level processes suggest that the upper tropospheric wave influence is most likely producing the stronger vertical motions.

TABLE OF CONTENTS

LIST OF TABLES

LIST OF FIGURES

ACKNOWLEDGEMENTS

For their significant contributions toward this thesis, I would like to extend my gratitude to the following people:

- To my advisor, Professor Carlyle Wash for his tolerance, patience and guidance in completing each challenging task of this thesis,
- To my second reader, Professor Russell Elsberry, for his outstanding editing and inspiration to produce the very best possible product,
- To Professor Dave Schrady, who made the statistical portion of this thesis understandable and graciously guided the author through some difficult statistical testing,
- To Professor Robert Renard, for the benefit of having his professional critique and important suggestions,
- To Paul Dobos, for his timely assistance, and extra effort to modify the mass and circulation budget computer programs for the new FGGE data,
- To my fellow classmate Sinclair Harris, for his valuable instruction on the use of GRAFSTAT and assistance in preparing the statistical sections of this thesis,
- Most especially I would like to thank my loving wife, June, for her undying support, patience and prayers.

I. INTRODUCTION

Rapid cyclone development in maritime regions of the world poses a particularly dangerous threat to today's mariner. These explosive cyclogenesis events are defined as low pressure systems with a deepening rate of one mb per hour for a 12 h period or longer. They are primarily maritime events with a maximum occurrence in the western oceans. Current operational forecast methods have been unreliable in accurately predicting the development of these types of storms (Sanders, 1987). The difficulty in forecasting these systems is due to their often small scale, their rapid deepening rate and the lack of in-situ data in the ocean environment.

Two recent examples of rapid cyclogenesis events discussed in the literature are: the Presidents' Day cyclone (18-20 February 1979) by Bosart (1981), Bosart and Lin (1984) and Uccellini et al. (1984, 1985); and the Queen Elizabeth II storm (9-11 September 1978) by Gyakum (1983a,b), Anthes et al. (1983) and Uccellini (1986).

Bosart and Lin's (1984) study of the Presidents' Day snow storm illustrated the importance of the planetary boundary layer processes and cold air damming to the east of the Appalachians for explosive cyclogenesis. Uccellini et al. (1984) discussed the importance of unbalanced flow in the subtropical jet near the eastern seaboard that resulted in coupled indirect vertical circulations. In this scenario, the low-level jet in the lower branch of this circulation aided in the development of precipitation even though the trough axis was farther upstream.

The Queen Elizabeth II storm development was originally attributed to latent heat release by Gyakum (1983a). In this case, Gyakum asserted that the storm developed in an environment in which baroclinic support was confined to the lower troposphere. However, Uccellini (1986) pointed out that there were important upper-level baroclinic processes upstream of the rapidly developing cyclone. Twelve hours prior to the rapid cyclogenesis, a short wave trough was located 400 to 500 km. Associated with the trough was:

- a polar jet marked by maximum winds of 65 m/s and significant vertical and horizontal wind shear;
- positive vorticity advection and divergence at the 300 mb level; and
- an intense front from the 300 mb level to the surface.

The physical processes involved in the rapid deepening of cyclones are still being studied. There are two primary views on the physics of explosive cyclogenesis. The first approach by Bosart (1981) and Gyakum (1983a,b) emphasized the low-level baroclinic environment and the convective bulk heating effects to explain the cyclone development. In addition, Rogers and Bosart (1986) documented that the explosive deepening cyclone resulted from a shallow baroclinic system with weak vertical stability near the center.

The second approach by Uccellini et al. (1985) and Wash et al. (1988) concentrated on the upper tropospheric jet and wave structures. In this case, the rapid cyclone development was related to the interaction between diabatic and dynamical processes in the troposphere, including the strength of the upper-level jet and its ageostrophic circulation, and the static stability of the marine boundary layer.

A statistical study of many explosive and nonexplosive cyclones during the period, 17 January to 23 February 1979 was conducted by Smith (1986). This study of 14 explosive and 14 nonexplosive cyclones concentrated on upper-level forcing mechanisms and boundary layer characteristics during the initial rapid deepening periods. Diagnostic calculations for both storm groups were compared. His evaluation of storm environment parameters suggested upper-level support was important in the deepening process. In the explosive cases, the positive vorticity advection, eddy mode of vorticity transport and the upper-level divergence were significantly greater than in the nonexplosive cases. However, other important factors, such as the low-level baroclinicity, were not thoroughly investigated.

The intent of this research is to evaluate explosive maritime cyclogenesis using the new, revised First Global GARP Experiment (FGGE) analyses (Paegle, 1986). The main objectives of this thesis are to:

- update the collection of explosive and nonexplosive cyclones of Smith (1986), using the enhanced FGGE analyses;
- evaluate a number of cyclone diagnostic terms to study storm intensity, low-level baroclinicity, static stability and upper tropospheric processes for the explosive and nonexplosive cases; and
- statistically determine dynamical differences between explosive and nonexplosive cyclogenesis.

In this study, the quasi-Lagrangian or storm following budgets discussed by Johnson and Downey (1975a,b) are used to determine the cyclone's properties and transports. The cyclone development is related to the dynamical and thermodynamic processes in the upper and lower troposphere. The horizontal and vertical mass circu-

lation is directly proportional to the amount of low-level convergence and upper-level divergence. The mass budget analysis describes this vertical and horizontal transport. The important features of upper-level forcing that are evaluated include positive vorticity advection, mass divergence and the thermal structure, whereas the absolute vorticity and the degree of reduced static stability ($d\theta/dp$) of the lower troposphere are also compared.

This thesis is organized into seven chapters. The second chapter reviews applicable literature on explosive cyclogenesis. Chapter Three concentrates on the methods of data assimilation and analysis of FGGE data. The separation of explosive and nonexplosive cyclones will be described in Chapter Four. The application of the quasi-Lagrangian diagnostic technique to this data set will be described in Chapter Five. Chapter Six provides a statistical comparison of the two storm groups. The last chapter summarizes the results of this research and offers recommendations to improve studies of explosive cyclogenesis.

II. LITERATURE REVIEW

The physical processes thought to be responsible for explosive cyclogenesis are latent or sensible heating, low-level baroclinity, upper-level perturbations and symmetric instability. The roles of these events are presented in this chapter by examining current literature.

Sanders and Gyakum (1980) focused attention to the problem of rapid maritime cyclone development. Because these low pressure systems form quickly and are frequently intense they represent a potentially dangerous environment for mariners. Sanders and Gyakum compiled a synoptic dynamic climatology during the period from September 1976 to May 1979. They concluded that rapid cyclogenesis was primarily a maritime event with maximum occurrence in the western oceans. The most frequent regions of formation were within or just north of the Gulf Stream and Kuroshio currents. In the Aleutian and Icelandic low regions, there was a noticeable lack of explosive cyclogenesis formation. One of the primary results of their study was that these events tend to occur in regions with the largest sea-surface temperature gradients.

The development scenario proposed by Sanders and Gyakum (1980) was one with cold polar air moving over the warmer ocean, which results in destabilization of the lower atmosphere. This process includes the convection and latent heat release in an environment of reduced static stability playing an important role in rapid cyclone development. In addition, the upper-level vorticity advection and low-level baroclinity were thought to be key elements in the development process.

Uccellini (1986) investigated the role of upper-level baroclinic processes in rapid cyclogenesis. An analysis of the Queen Elizabeth II (QE II) storm of 9-11 September 1978 revealed the presence of upper level baroclinic processes upstream of the developing cyclone. Specifically, a deep frontal zone associated with a short wave trough and polar jet were positioned upstream. The baroclinic processes associated with the system could have aided in rapid cyclogenesis. The upper-level pattern included a short wave trough and a polar jet with maximum winds of 65 m/s and significant vertical and horizontal wind shear. At the upper level (300 mb), positive vorticity advection and divergence were present, in addition to an intense frontal zone at the low level (800 mb). A tropopause fold brought upper tropospheric air down to the 700 to 800 mb levels prior

to the rapid development phase of the cyclone. This study clearly showed that upper-level forcing was a key ingredient in the development of the QE II storm.

A thorough synoptic investigation of frontal wave cyclogenesis in the North Atlantic and North Pacific Oceans was conducted by Wash et al. (1988). Two cases of explosive cyclogenesis were evaluated using the European Centre for Medium-range Weather Forecasts (ECMWF) objective analyses during FGGE. The first case involved the development of a cyclone on a frontal baroclinic zone in the western North Pacific Ocean. The incipient cyclone formed due to the surface convergence between an extreme cold outbreak and warmer tropical air. Reduced static stability was caused by sensible heating of the lower troposphere by a warmer ocean. This resulted in decreasing the braking tendency due to vertical motions and upper-level divergence. The second case involved the formation of a polar low in the North Atlantic Ocean region. In both cases, strong upper-level support was present in the form of an intense jet streak that aided in the explosive deepening of the cyclone. The positioning of the divergence region of the upper-level jet greatly enhanced the vertical motion and low-level convergence associated with the storm development. When the cyclone moved north of the jet in the North Pacific Ocean case, the decreased upper-level support resulted in slower development of the storm. The results of this study suggested that upper-level forcing was a key element in the initiation of explosive oceanic development. This agreed with previous papers by Uccellini et al., who concentrated on the role of the upper tropospheric jet and wave structures. However, reduced stability in the lower troposphere certainly aided the baroclinic environment necessary to rapidly develop a cyclone.

In contrast to the Uccellini et al. and Wash et al. analyses, Pagnotti and Bosart (1984) emphasized the role of the low-level baroclinic environment and the convective bulk heating effects on rapid cyclone development during the Presidents' Day storm (18 February 1979). Significant features of this storm were the boundary layer warming and the relatively large moisture flux. The important physical mechanisms in the development of the incipient cyclone were differential heating, moistening and differences in topography between the land and sea, in addition to the cold air being dammed against the Appalachian Mountains. Rapid deepening occurred when the upper-level southwesterly flow was positioned over the cyclone. The convergence of moisture flux in the surface to 700 mb layer intensified and expanded eastward. In the coastal boundary layer, convergence of the water vapor dominated the horizontal advection of moisture. This was a vital factor in the development of the large amount of precipitation that accompanied this storm. The latent and oceanic sensible heat fluxes demonstrated that the

boundary layer processes were critical in the development of the storm. The onshore wind flow was also a key element in the resulting frontogenesis and cyclogenesis. This provided the additional support for the important ageostrophic circulation as a precursor for later development.

The Presidents' Day and QE II storms are obviously related to the dynamic and diabatic processes over the entire troposphere. However, the role of upper-level forcing can have a variable nature. The position of the upper-level jet streak and the stability of the air are critical factors in rapid cyclogenesis. Therefore, the determination of the vertical and horizontal structure of the atmosphere is important to this evaluation.

Rogers and Bosart (1986) examined the three-dimensional structure of cyclone development using rawinsonde data. The four stages of the cyclone were defined as:

- Incipient. The initial formation of a low pressure area as analyzed by the National Meteorological Center. This period included the beginning of the cyclone until the start of the rapid deepening rate.
- Explosive. The period with a deepening rate of at least one mb per hour for 12 to 24 h.
- Mature. The period in which the rapid deepening rate ends, and the central pressure and areal extent of the cyclone's circulation remain quasi-steady.
- Decaying. During this segment there is a significant increase in the storm's central pressure with an associated decrease in intensity.

This study evaluated the generation of an explosively deepening cyclone that originated in a shallow, lower tropospheric system. It subsequently evolved into a deep and intense vortex with a strong baroclinic signature. Other contributing factors included jet streak dynamics (Uccellini et al., 1984) and symmetric instability (Emanuel, 1983; Rogers and Bosart, 1986). The possibility of nonlinear interactions in the baroclinic instability process was also considered.

One of the methods used to evaluate rapid cyclogenesis was the quasi-Lagrangian diagnostic budget technique (Wash et al., 1988). This approach used a spherical coordinate system and transport equations described by Johnson and Downey (1975a,b). The motivation for using a budget analysis is the simplicity of describing the physical processes in terms of balancing the mass circulation inflow and outflow. The interactions between the budget volume and the environment are analyzed through the transport relationships based on the governing equations. This storm-centered budget approach provides a framework to composite the explosive and nonexplosive cases in this study.

The summary of this literature review is that the physical processes that accompany explosive cyclogenesis were varied and inconclusive. This thesis will focus on the upper-level forcing and the role of low-level baroclinity in rapid cyclogenesis. The specific areas of interest are:

- the nature of the favorable marine environment;
- the structure of low-level baroclinicity of the incipient cyclone; and
- the coupling between the upper and lower troposphere.

The relative magnitudes of these processes will be analyzed in detail to identify the most dominant feature in explosive cyclone development. The newest FGGE analyses are used to evaluate these elements. The next chapter explains the methods and techniques of data assimilation and analyses used in the FGGE processing.

III. DATA ASSIMILATION

The scarcity of data over open-ocean areas limits the study of maritime rapid cyclogenesis. The First GARP Global Experiment (FGGE) represented the first time a truly global data set has been prepared (Halem et al., 1982). This thesis uses the revised FGGE analysis data (Paegle, 1986). The sources for the FGGE data collection included surface (sea, land and drifting buoy) reports and rawinsondes. Additional data were provided from dropsondes, aircraft, pilot balloons and satellite measurements. The requirement for 500 km horizontal resolution was fulfilled by more than 7000 temperature sounding profiles per day and 6000 cloud drift winds from five geostationary satellites (Halem et al., 1982).

The European Centre for Medium-range Weather Forecasts (ECMWF) prepared analyses of the FGGE data set for the entire year. During the special observing periods (SOP's), the archiving was accomplished every 6 h, otherwise it occurred every 12 h. The analyses were performed for 19 levels in the vertical and with a horizontal resolution of 1.875° latitude longitude.

The processing and management of data were separated into three levels of control. Level I was comprised of primary data from a variety of instrumented platforms. Level II-b represented (where b denotes data collected from the global research data set) the transformation of Level I data into basic meteorological parameters (Bjorheim et al., 1981). The Level III-b data set contained both basic analysis parameters in addition to derived ones. The original analyses were not initialized and were comprised of geopotential height, sea-level pressure and horizontal wind components. The derived terms included temperature, relative humidity and vertical velocity at each vertical level (Bengtssen et al., 1982).

One of the primary differences between the main and final Level II-b data sets was the addition of world-wide synoptic and ship data, which more than doubled the original amount of data. The final data set also included additional aircraft reports, data from three monsoon experiments, the United States special effort satellite temperatures (SATEM's) and cloud-drift winds (SATOB's), a new set of SATOB winds produced by the University of Wisconsin from Japanese HIMAWARI imagery and from the METEOSAT for 06 and 18 UTC during SOP's, and reprocessed DROPSONDE data. (Uppala, 1986).

The initial data assimilation used to produce the Level III-b analyses consists of a multivariate optimum interpolation analysis, a nonlinear normal mode initialization, and a high resolution model that provided a first-guess forecast. The new ECMWF assimilation of the FGGE Level III-b data consists of the following changes (Shaw et al., 1987):

- diabatic nonlinear normal mode initialization;
- incorporation of a diurnal cycle and improved humidity analysis;
- greater vertical resolution in the upper levels;
- revision of the Optimum Interpolation (OI) statistics package; and
- a revision of the quality control criteria.

The present ECMWF spectral model with rhomboidal truncation and mean orography was used for the FGGE analyses. The revised physical parameterizations included a formulation of deep and shallow convection, as well as cloud and radiation schemes. Two previous weaknesses in the OI technique were the unrealistically low analyses error in data-rich areas and a high growth rate of forecast error for most regions. The solution to this problem has been to assume the revised growth rate is linear, which has resulted in agreement with statistical estimates. In addition, the new first-guess estimates are lower and similar to upper-level geopotential values. Another improvement in the new FGGE analyses was to increase the vertical resolution from 12 to 19 levels (the horizontal resolution remained at 1.875°).

The updated quality control methods have introduced checks to eliminate incorrect data inputs. Shaw et al. (1987) have described certain observational platforms that have consistently provided erroneous data. These platforms have been excluded in the new analyses. The ECMWF algorithm for generating the upper atmosphere background field for the 10, 20 and 30 mb analyses was improved to include upper-level wave effects. This modification was accomplished to include Rossby and Kelvin wave effects and to produce more reasonable height fields.

The comparisons of the initial and final data sets are still being performed. Preliminary results have shown changes up to ten mb in the Southern Hemisphere and four mb in the Northern Hemisphere oceans for a typical mean sea-level pressure pattern. The adjustment of wind data in the upper troposphere has been improved while the comparison at 400 mb is closer to the initial analysis due to the smaller assumed observational errors. Evaluations of ECMWF analyses have shown that greater weighting has been given to the more accurate data (e.g., pilot reports and aircraft data) when

available. In data sparse regions, i.e., across the open ocean, greater use of SATOB data has occurred.

There have been substantial improvements to the FGGE Level III-b data set produced by ECMWF. These improvements and the increased data availability have resulted in an appreciably higher quality analysis. The locations of rapid cyclogenesis and the calculations of storm environment parameters rely heavily on the accuracy of this data set. The progress made in developing the new FGGE data set should improve the outcome of this research. The following chapter concentrates on the selection of storms and the development of a list of rapid cyclogenesis cases.

IV. SCREENING AND SELECTION OF EXPLOSIVE AND NONEXPLOSIVE CYCLONES

The region of cyclone development was based on the studies by Smith (1986) and the previous cyclone climatology of the North Atlantic and Pacific Oceans (Sanders and Gyakum, 1980). The north-south boundaries (20°N to 60°N) were the same for the North Pacific and Atlantic Oceans. The east-west borders in the North Pacific Ocean, went from 170°W across the international dateline to 120°E. The east-west boundaries in the North Atlantic Ocean stretched from 40°W to 85°W. The period of the evaluation was from 17 January to 28 February 1979 as part of the first special observing period (SOP).

The initial screening of the storms was accomplished by Smith (1986) from sea-level pressure analyses produced by the National Meteorological Center. The criterion for selection of a cyclone was a closed isobar throughout the initial 24 h development period. The requirement for an explosive cyclone was a deepening rate of at least one mb per hour for a time period of 12 to 24 h. Cyclones that deepened at a lesser rate were classified nonexplosive. The deepening rate was adjusted for latitude by the correction factor $\sin\theta / \sin 60°$, where θ was taken at the point of the most rapid deepening. This adjustment factor normalized the pressures for 60° latitude. In addition, only storms that deepened over oceanic waters were considered. Storms that regenerated after an initial deepening were not included due to other physical processes being responsible for their formation.

The storm tracks in the North Atlantic and Pacific Oceans are displayed in Figs. 1 and 2. As previously mentioned, favorable areas of explosive and nonexplosive cyclone generation are located near the western ocean boundary currents. In the North Pacific Ocean, most of the storms occlude and move off to the northeast before reaching the international dateline. In the North Atlantic Ocean, the storm tracks are more dominant off the east coast of the United States, which poses a particularly dangerous threat to vessels in the maritime shipping lanes. The most severe storms formed in a 400 to 500 n mi radius from Cape Hatteras, North Carolina.

The initial list compiled by Smith (1986) was revised based on the new FGGE sea-level pressure analyses. The results of this revision for the North Pacific Ocean are as follows:

- shifted the development positions of the explosive cyclones P1, P5, P6, P7, P8 and the nonexplosive cyclones NP1, NP8, NP9, NP11;
- started storms P4, P7, P8, NP1, NP9 and NP11 12 h earlier;
- started storms NP6 and NP10 12 h later;
- shifted NP9 and NP11 to the explosive category,
- designated P4 and P8 as rapid deepening storms for only 12 h; and
- dropped NP4, NP5 and NP7 from the storm list due to pressure actually increasing vice decreasing (discovered in the new FGGE data).

In the North Atlantic Ocean, the following revisions were made:

- shifted the development locations for storms A1, A3, A4, A6, A7, A8 and NA2;
- started storm A1 12 h earlier;
- dropped NA3 from the storm list due to pressure actually increasing vice decreasing (discovered in the new FGGE data); and
- noted that A3 development was influenced by land vice maritime processes.

Listings of the explosive (A or P) and nonexplosive cyclones (NA or NP) in the North Atlantic and Pacific Oceans and their 0, 12 and 24 h positions are provided in Tables 1 and 2. The total deepening for the 12 and 24 h periods are listed in Tables 3 and 4. In addition, Tables 5 and 6 provide a listing of the changes in the sea-level pressure (ΔP) for each 12 h period. Wherever possible, *the center of a closed isobar* was used to begin the initial development stage. In other cases, explosive development occurred so rapidly that the 12 h predevelopment did not show a closed isobar. In those cases, ridging in the 500 to 1000 mb thickness pattern and the general structure of the surrounding isobars were used to locate the center.

The results in Tables 1 through 4 indicate that storm development near the western ocean boundary currents is quite dominant. The frequency of explosive and nonexplosive cyclone development in this 42-day sample generally agrees with the previous studies (Sanders and Gyakum, 1980) in that the North Pacific Ocean has more storms but the North Atlantic Ocean cyclones have a larger deepening rate. Tables 1 through 6 list 16 explosive (including the one that formed over land) and the eight nonexplosive storms. The cyclones that deepened for only 12 h and the ones that were not formed over the ocean environment were excluded in further statistical analyses.

The next chapter discusses the development and usage of the mass and circulation budgets. These methods will produce the data necessary to determine the most dominant characteristics in the process of cyclogenesis.

Table 1. EXPLOSIVE CYCLONE POSITIONS IN THE NORTH PACIFIC AND ATLANTIC OCEANS, FROM ECMWF ANALYSES, 1979. * denotes storms with 12 h of deepening, ** denotes initial development over land and time is in UTC.

EXPLOSIVE STORMS	STORM POSITIONS FOR PACIFIC AND ATLANTIC OCEANS			
	START TIME	0 HOUR	12 HOUR	24 HOUR
PACIFIC OCEAN	DDMMHR	POSITION	POSITION	POSITION
P1	18JAN00	40.2N 139.1E	39.5N 147.7E	42.2N 157.2E
P2	26JAN00	32.6N 145.5E	31.0N 160.0E	30.0N 168.0E
P3	05FEB12	31.5N 134.0E	36.0N 141.0E	42.0N 146.0E
P4 *	10FEB00	49.0N 163.0E	50.5N 167.0E	-
P5	17FEB12	37.5N 141.5E	39.3N 149.0E	43.0N 158.0E
P6	15FEB12	39.0N 144.0E	42.5N 152.0E	48.0N 155.0E
P7	25JAN12	39.0N 174.0E	40.0N 179.0E	45.0N 179.0W
P8 *	28JAN00	38.0N 160.5E	40.0N 166.5E	-
P9	19FEB00	43.0N 148.0E	40.5N 152.0E	44.0N 160.5E
ATLANTIC OCEAN	DDMMHR	POSITION	POSITION	POSITION
A1	18JAN00	45.0N 070.0W	41.8N 064.3W	40.0N 060.0W
A3 **	28JAN00	38.0N 082.0W	37.0N 072.0W	39.5N 063.0W
A4	31JAN12	33.0N 080.0W	35.0N 071.0W	38.0N 063.5W
A5	10FEB00	33.5N 070.0W	38.0N 056.0W	42.0N 045.0W
A6	13FEB00	37.0N 080.0W	35.5N 068.0W	39.0N 055.0W
A7	19FEB00	31.5N 077.5W	36.0N 075.0W	37.5N 067.5W
A8	15FEB00	40.0N 053.0W	47.5N 040.0W	54.0N 035.0W

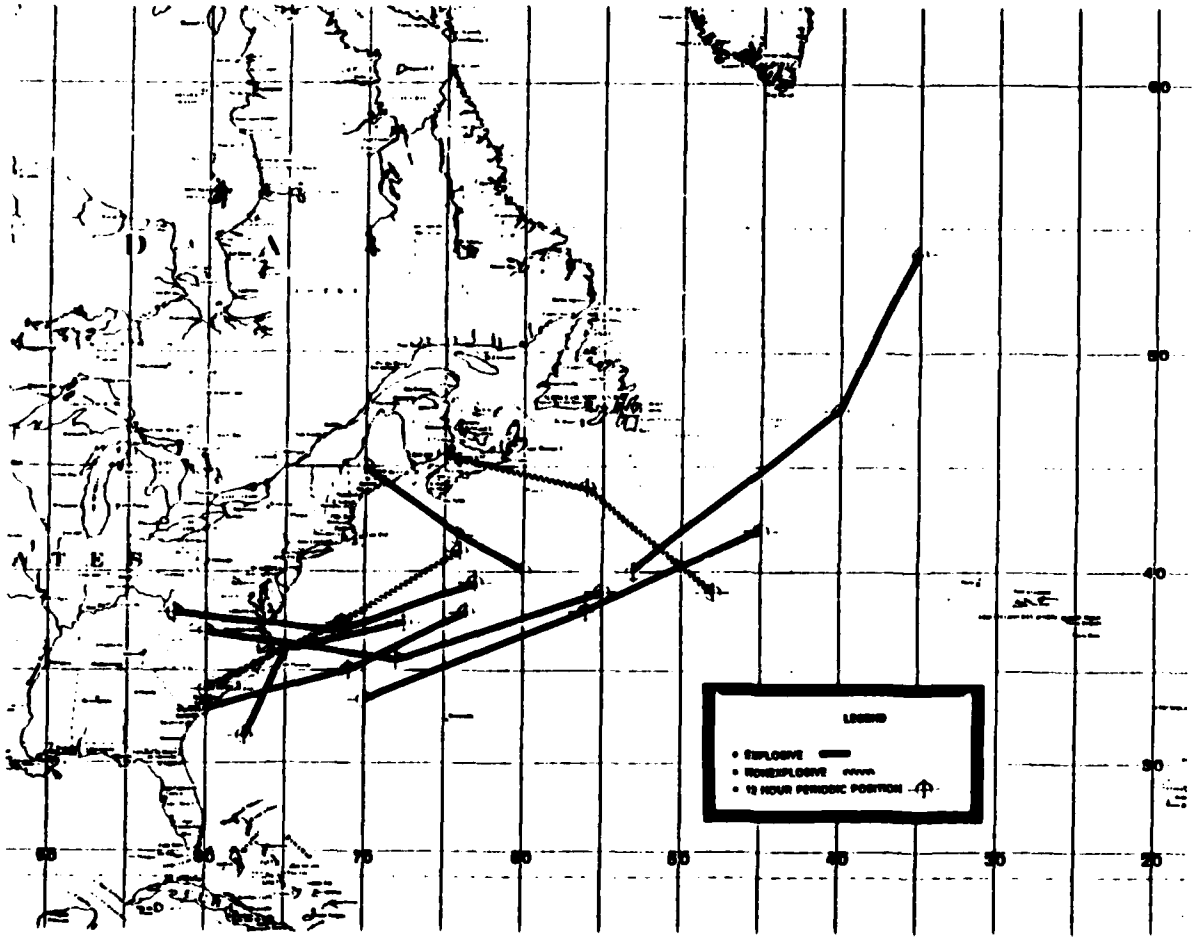

Figure 1. North Pacific Ocean storm tracks and positions for a 24-h interval.

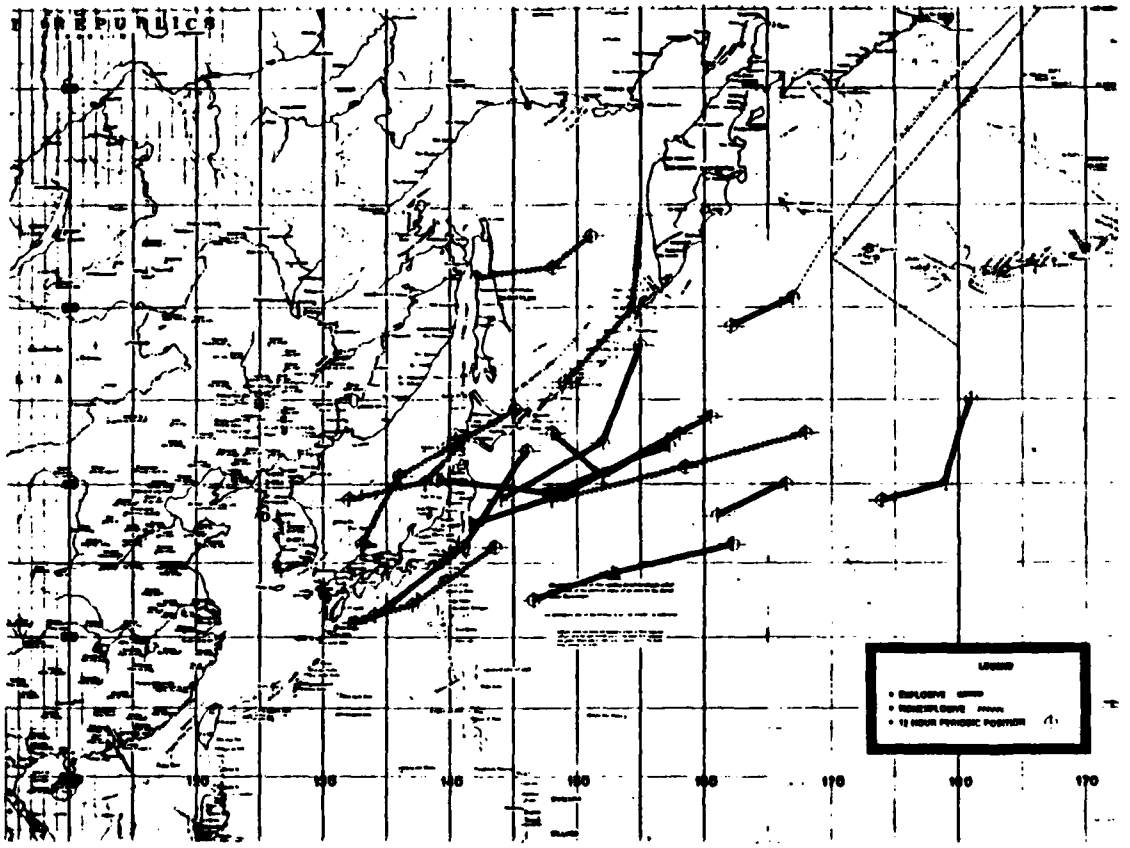

Figure 2. North Atlantic Ocean storm tracks and positions for a 24-h interval.

Table 2. NONEXPLOSIVE CYCLONE POSITIONS IN THE NORTH PACIFIC AND ATLANTIC OCEANS, FROM ECMWF ANALYSES, 1979. Time is in UTC.

NONEX-PLOSIVE STORMS	STORM POSITS FOR PACIFIC AND ATLANTIC OCEANS			
	START TIME	0 HOUR	12 HOUR	24 HOUR
PACIFIC OCEAN	DDMMHR	POSITION	POSITION	POSITION
NP1	21JAN12	39.0N 148.0E	41.0N 158.5E	43.0N 168.0E
NP2	31JAN12	36.1N 133.0E	40.5N 136.0E	44.5N 145.1E
NP3	04FEB12	46.0N 149.0E	50.0N 154.5E	54.5N 155.0E
NP6	13FEB12	31.0N 132.4E	32.3N 137.0E	36.0N 143.5E
NP8	21FEB00	51.5N 142.0E	52.0N 148.0E	53.5N 151.0E
NP9	13FEB12	39.0N 132.0E	40.0N 139.0E	42.5N 141.0E
ATLANTIC OCEAN	DDMMHR	POSITION	POSITION	POSITION
NA1	07Feb12	34.0N 080.0W	37.5N 071.5W	41.0N 064.0W
NA2	22FEB12	45.5N 065.0W	44.0N 056.0W	39.0N 048.0W

Table 3. PRESSURE VARIATIONS FOR EXPLOSIVE CYCLONES IN THE NORTH PACIFIC AND ATLANTIC OCEANS, FROM ECMWF ANALYSES, 1979. * denotes storms with 12 h of deepening, ** denotes initial development over land and time is in UTC.

EXPLOSIVE STORMS	STORM PRESSURE VARIATIONS			
	START TIME	0 HOUR	12 HOUR	24 HOUR
PACIFIC OCEAN	DDMMHR	PRESSURE(MB)	PRESSURE(MB)	PRESSURE(MB)
P1	18JAN00	1006	985	970
P2	26JAN00	1010	998	989
P3	05FEB12	1015	1006	992
P4 *	10FEB00	1003	992	-
P5	17FEB12	1006	985	977
P6	15FEB12	997	989	977
P7	25JAN12	995	984	975
P8 *	28JAN00	995	980	-
P9	19FEB00	1002	994	985
ATLANTIC OCEAN	DDMMHR	PRESSURE(MB)	PRESSURE(MB)	PRESSURE(MB)
A1	18JAN00	1017	1003	988
A3 **	28JAN00	1001	992	978
A4	31JAN12	1012	999	980
A5	10FEB00	1007	996	973
A6	13FEB00	1014	1006	992
A7	19FEB00	1021	1015	993
A8	15FEB00	995	987	973

Table 4. PRESSURE VARIATIONS FOR NONEXPLOSIVE CYCLONES IN THE NORTH PACIFIC AND ATLANTIC OCEANS, FROM ECMWF ANALYSES, 1979. Time is in UTC.

NONEX-PLOSIVE STORMS	STORM PRESSURE VARIATIONS			
	START TIME	0 HOUR	12 HOUR	24 HOUR
PACIFIC OCEAN	DDMMHR	PRESSURE(MB)	PRESSURE(MB)	PRESSURE(MB)
NP1	21JAN12	1005	1000	997
NP2	31JAN12	1009	1000	996
NP3	04FEB12	1009	1005	1003
NP6	13FEB12	1015	1010	1003
NP8	21FEB00	999	991	985
NP9	13FEB12	1013	1007	1005
ATLANTIC OCEAN	DDMMHR	PRESSURE(MB)	PRESSURE(MB)	PRESSURE(MB)
NA1	07Feb12	1006	1001	996
NA2	22FEB12	1008	1006	1000

Table 5. PRESSURE DECREASES OF EXPLOSIVE CYCLONES IN THE NORTH PACIFIC AND ATLANTIC OCEANS, FROM ECMWF ANALYSES, 1979. * denotes storms with 12 h of deepening, ** denotes initial development over land and time is in UTC.

EXPLOSIVE STORMS	STORM PRESSURE DECREASES (ΔP)		
	START TIME	AFTER 12 HOURS	AFTER 24 HOURS
PACIFIC OCEAN	DDMMHR	PRESSURE(MB)	PRESSURE(MB)
P1	18JAN00	21	15
P2	26JAN00	12	9
P3	05FEB12	9	14
P4 *	10FEB00	11	-
P5	17FEB12	21	8
P6	15FEB12	8	12
P7	25JAN12	11	9
P8 *	28JAN00	15	-
P9	19FEB00	8	9
ATLANTIC OCEAN	DDMMHR	PRESSURE(MB)	PRESSURE(MB)
A1	18JAN00	14	15
A3 **	28JAN00	9	14
A4	31JAN12	13	19
A5	10FEB00	11	23
A6	13FEB00	8	14
A7	19FEB00	6	22
A8	15FEB00	8	14

Table 6. PRESSURE DECREASES OF NONEXPLOSIVE CYCLONES IN THE NORTH PACIFIC AND ATLANTIC OCEANS, FROM ECMWF ANALYSES, 1979. Time is in UTC.

NONEXPLOSIVE STORMS	STORM PRESSURE DECREASES (ΔP)		
	START TIME	AFTER 12 HOURS	AFTER 24 HOURS
PACIFIC OCEAN	DDMMHR	PRESSURE(MB)	PRESSURE(MB)
NP1	21JAN12	5	3
NP2	31JAN12	9	4
NP3	04FEB12	4	2
NP6	13FEB12	5	7
NP8	21FEB00	8	6
NP9	13FEB12	6	2
ATLANTIC OCEAN	DDMMHR	PRESSURE(MB)	PRESSURE(MB)
NA1	07Feb12	5	4
NA2	22FEB12	2	6

V. MASS AND CIRCULATION BUDGET ANALYSIS OF THE CYCLONE DEVELOPMENT

The quasi-Lagrangian diagnostic technique (Wash, 1978; Johnson and Downey, 1975a,b) is used to evaluate cyclone development, maturation and dissipation for these groups of explosive and nonexplosive storms. The primary objective of the storm-following method is to analyze cyclone development within the westerly wave regimes of the midlatitudes. The computations are performed in a spherical coordinate system that translates with the storm. This system divides the lateral transport and advection associated with the wave translation from the quantities relative to the moving cyclone. The proper positioning of the budget volumes is a vital factor in obtaining meaningful results from these calculations.

The volume of the environment is centered on the lowest sea-level pressure from the surface analysis. A reference radius is constructed from the center of the cyclone to the center of the earth. The radius of the volume around the storm is separated into one degree latitude increments. This configuration is a cylindrical volume since the radius of the earth is much larger than the depth of the atmosphere.

The advantages of using this method are:

- focuses in on the key elements of development for a particular cyclone;
- evaluates the measure of the parameters responsible for development with respect to the cyclone centers; and
- quantitatively analyzes the development through the budget and transport relationship.

The equations used to describe the mass and vorticity circulation budgets are defined in Appendix A. The outputs of these calculations are used to determine the magnitude of the following key cyclone development terms:

- changes in central and areal average pressure;
- absolute vorticity;
- vertical velocity;
- low-level baroclinicity;
- layer-averaged potential temperature;
- static stability;
- vorticity advection;

- eddy mode of vorticity transport;
- mean mode of vorticity transport; and
- upper-level divergence.

The goals of these budgets were to measure the strength of cyclogenesis, and the degree of upper- and lower-tropospheric influences. The absolute vorticity, kinematic vertical velocity and changes in central and areal pressures are used to evaluate the strength of the cyclogenesis. The vorticity advection, eddy and mean modes of the vorticity transport, and upper-level divergence are evaluated for upper tropospheric influences. The upper-level divergence is measured by integrating the mass transport directed out of the budget volume in the upper troposphere. Finally, the static stability, layer-averaged potential temperature and low-level baroclinity are examined for low-tropospheric effects.

The mean and eddy modes comprise the horizontal transport of absolute vorticity. The lateral transport of absolute vorticity by the eddy mode strongly correlates with the vorticity advection (Calland, 1983). The boundary flux, the mean absolute vorticity and the normal component of the mean wind at two adjacent levels were used to determine the layer-average mean mode vorticity. The eddy mode was computed by subtracting the mean mode from the total absolute vorticity transport. The total transport was defined as the boundary flux of the product of the absolute vorticity and the normal component of the wind (Wash, 1978).

The kinematic vertical velocity was obtained from the vertically-integrated continuity equation in pressure coordinates. The divergence was computed by determining the vertical flux of mass at each level (assuming zero at the top and bottom boundaries). The lateral flux of mass was calculated from the wind fields and was balanced by the vertical flux to maintain conservation of mass. Unfortunately, errors in wind measurements resulted in the occurrence of a residual when the horizontal and vertical fluxes were compared. The O'Brien (1970) correction scheme was utilized to distribute these residuals. The weighting of this adjustment increased at the upper atmospheric levels since the winds were more difficult to measure at higher heights.

Several methods to measure the strength of the low-level baroclinicity were considered. Vertically averaged temperature differences at the storm boundary on a radial through the cyclone center were measured. The following different radials were considered when evaluating this term:

- a radial perpendicular to storm motion;

- a radial through the storm center from the warmest area in the warm sector; and
- a radial through the storm center to the coldest point north or northwest of the cyclone.

The maximum temperature difference from the warmest point along a radial through the storm center was chosen as the best technique due to its consistency and reproducibility. In general, this radial was the same radial perpendicular to the storm's motion. The largest temperature differences through the cyclone were also found along this radial. This temperature difference was a measure of the strength of the low-level frontal zone or baroclinity. The static stability was derived from the 1000 to 500 mb temperature analyses by the ECMWF.

Results of the computations of these cyclone development parameters are included in the next chapter. The results highlight the major differences in the storm environment properties between the explosive and nonexplosive groups.

VI. RESULTS

A. INTRODUCTION

In this chapter a statistical evaluation of the thirteen explosive and eight nonexplosive cyclones was conducted. The two explosive storms that deepened for only 12 h and the explosive storm that formed over land were excluded from this statistical study. Smith (1986) previously prepared statistics on upper- and low-level cyclone development processes. This study uses the new FGGE analyses and focuses on assessing the significance of the terms responsible for explosive cyclogenesis. These terms, introduced in Chapter Five, were compared for the 24 h cyclogenesis period and at the different time intervals (0, 12 and 24 h). The evaluation of these parameters was performed in the storm-centered framework using averages from 4° and 6° latitude radii budget volumes. Hereafter, these volumes will be referred to as 4° / 6° radii volumes.

Statistical box plots provide a convenient method to display the variations in data distribution using quartiles. The change in pressure (ΔP) shown in Fig. 3 is used as an example. The first two plots (going left to right) are at the 12 h changes in pressure for the explosive and nonexplosive storms. The two plots on the right are for the 24 h time period. The medians (horizontal line segment within the box) for the 12 h period. are 11 mb for the explosive cyclones and 5 mb for the nonexplosive ones. The top of the box for the explosive storms at the 12 h period represents the 75 percentile (13 mb) and the bottom is the 25 percentile (8 mb). The interquartile range (Q) is the distance from the bottom of the box to the top (Chambers et al., 1983). The value of Q is used to define the following terms:

- adjacent values are within 1.5Q of the quartiles;
- outside points are between 1.5 to 3Q of the quartiles; and
- detached points are greater than 3Q away from the quartiles.

The clear separation of the explosive and nonexplosive 24 h pressure changes in the box plots reflects the rapid development definition of the two cyclone groups from the sea-level pressure maps.

The box plots allow a partial assessment of symmetry. If the distribution is symmetric, then the box plot is symmetric about the median. Additionally, if the distance to the upper adjacent point from the top of the box is greater than the lower distance

from the bottom, then the data distribution is skewed to the higher pressure, as in the case of the explosive storms (for the 12 h mark in Fig. 3). The explosive storms have a higher mean (represented by a circle) and median than the nonexplosive ones, following the definition of the groups. The variability of the data for the explosive storms is greater during both time periods which can be observed in Tables 5 and 6 (Chapter 4). This graphical representation provides a method to compare average values and also the distribution of the data set.

The Kolmogorov-Smirnov test for goodness of fit was performed to determine if the individual terms are normally distributed (Appendix B contains a more detailed description of this process). If the data were normally distributed, then a student t-test and 90 percent confidence level were calculated to determine the statistical relationships between the storm groups. Those storms that met the critical test statistic value for rejecting the hypothesis (that the means were equal) at a significance level of ten percent are denoted by a subscript 't' in the following tables. The degree of difference was a function of the sample size and the size of the standard deviations (Devore, 1987). The standard deviations are included in parentheses next to the mean values in Tables 7 through 18 for for the upper-level and low-level forcing functions.

The time tendency and 24 h evolution of upper-level and low-level forcing terms are displayed in Figs. 4 through 21. The inner two plots (going left to right) correspond to the explosive and nonexplosive storms at 4° latitude radius and the outer plots at 6° radius. These figures are for the initial, 12 and 24 h time intervals.

B. TIME TENDENCY OF LOW-LEVEL CIRCULATION

The terms that describe the strength of the cyclogenesis process are associated with the low-level absolute vorticity and vertical motion. The strength of the low-level circulation was measured by comparing the absolute vorticity for the 1000 to 850 mb level. The initial values for the nonexplosive storms were higher by about ten percent as shown in Table 7. Several explosive storms developed so rapidly that no closed isobar are present at the initial time. The inclusion of these systems likely explains the higher initial low-level vorticity values in the nonexplosive set and the large vorticity increases in the explosive set. The fact that the initial values were less for the explosive cases indicated that the low-level intensity was not the initial dominant factor in the separation of explosive and nonexplosive storm development.

As the storm development progressed, the explosive cyclones exhibited a larger absolute vorticity increase and final 24 h value averaged over 4° latitude radius. The 24 h

value is the only statistically different absolute vorticity between the explosive and non-explosive samples, compared to other radii and time periods (Table 7). The higher values of absolute vorticity at the initial time for the nonexplosive cyclones suggests that separating the storm groups using these initial values is impossible. The greater absolute vorticity at the 4° radius for the explosive storms is shown in Figs. 4 through 6 (as time increased to the 24 h point). This indicates a tighter pressure gradient and a more organized storm in the explosive cases, in agreement with the central pressure statistics.

The absolute vorticity of the nonexplosive cyclones for the 6° radius volume was larger than the explosive storms by ten percent at the start of the cyclone development. During the 24 h development period for the explosive storms, the 6° latitude vorticity values do increase more than the nonexplosive storms, but not as dramatically as for the 4° volume. At the 24 h mark, the average vorticity values are similar for the two groups. This indicates that the explosive storms are more compact with an intense inner core, but the average vorticity does not differ from the nonexplosive storms using the 6° radius volume.

C. TIME TENDENCY OF VERTICAL MOTION

The sample statistics for the 850 mb and 700 mb kinematic vertical velocities (units of 10^{-4}mb sec) at 4° and 6° latitude radii are listed in Tables 8 and 9. Figs. 7 through 9 are the box plots of the vertical velocity for each time interval. The key results from the tables are the statistical separation of vertical motion for the 4° and 6° radii volumes at the start of cyclogenesis. This indicates a significant upward vertical motion in the early stages of storm development. The maximum vertical velocity occurs at the 12 h point for all other radii and time periods.

Kinematic vertical motion values at 4° radius, for explosive cyclones are greater than the nonexplosive ones for all three time periods. The two groups are statistically separable for the 0 h and 24 h periods. After 12 h, the variability of the vertical motion for the nonexplosive storms is quite large. This is shown by the sizeable standard deviations in Table 8 and the range of values on the box plots in Fig. 8. Consequently, this time period did not pass the statistical test.

The results of the 4° radius vertical motion are also reflected for the 6° volume. Significantly larger kinematic vertical motion values are present for all time periods for the explosive storms. The 850 mb vertical motion values are statistically separable for all time periods, while the 700 mb vertical motion is separable at the 0 h and 12 h mark.

The stronger vertical motion values at both the 4° and 6° radii and at most of the time periods indicates the explosive set is characterized by vigorous upward vertical motion that is present at the start of sea-level cyclogenesis. These large vertical motion values are consistent with the strong vorticity increases and pressure falls shown earlier.

In addition to the kinematic vertical velocities, vertical velocities from the ECMWF analyses were also studied. Cyclone-centered averages (not shown) from the ECMWF vertical motions were considerably more variable in time than the kinematic vertical motions. The ECMWF vertical motion results were inconsistent with the behavior of the cyclones studied. This suggest inaccuracies in the normal mode initialization of the ECMWF analyses, perhaps caused by a smoothing of the initial vertical velocities.

D. TIME TENDENCY OF STATIC STABILITY

The static stability is evaluated in the layer of 1000-500 mb (Tables 10 and 11). The results show both explosive and nonexplosive systems develop in a weak static stability environment. However, statistical separation between the groups only occurred for the 6° radius case at the 12 h point. The similarity in the standard deviations and means for both storm groups suggest that the low-level environment was basically the same for the explosive and nonexplosive cyclones.

Static stability values ($d\theta$ dP) for the explosive storms are 0.2 K/100 mb to 0.5 K/100 mb less than the nonexplosive storms (Tables 10 and 11). This agrees with the expected reduced static stability for the more rapid deepening storms. However, the initial static stability analyses, like the initial low-level vorticity, can not be used to separate the nonexplosive from explosive cyclone groups. Although the average static stability is similar for the explosive and nonexplosive cyclones, there still may be particular quadrants or regions of the cyclone for which there are large static stability differences. Quadrant analyses were not conducted in this study but should be investigated in the future.

E. TIME TENDENCY OF LOW-LEVEL BAROCLINITY

The low-level baroclinic structure is specified from 1000-800 mb and 1000-500 mb temperature differences across the frontal zone. Specifically, the temperature values through the warmest sector and usually perpendicular to the storm motion are considered. The explosive storm temperature differences are slightly larger than their counterparts as shown in Tables 10 and 11. However, the differences between the storm groups are within a standard deviation, and statistical separation is impossible.

The frontal zone strength does not change appreciably during the 24 h development period. However, the frontal zone does show a tendency to strengthen for the first 12 h. The largest gradients for the explosive and nonexplosive cases occurred at the 12 h point with the exception of the 6° latitude radius explosive cyclones at the 1000 to 800 mb layer (Tables 10 and 11). Overall, the 1000-500 mb values had lower standard deviations compared to the 1000-800 mb level. This suggests that there is less variability in temperature values when including the layer between 800-500 mb. This is consistent with the storm-to-storm variations being less when evaluating temperature changes through a deeper layer of the troposphere. The results of this term show that the strength of the low-level frontal zone does not differ significantly between the explosive and nonexplosive groups.

F. TIME TENDENCY OF UPPER-LEVEL FORCING

The strength of the upper-level forcing was estimated from the averaged (500 to 200 mb) vorticity advection, the eddy and mean modes of vorticity transport, and the upper-level divergence. Major differences between rapid and normal cyclogenesis at the initial period are found in the upper-tropospheric results. Averaged over 4° latitude radius (Table 12), the upper-tropospheric comparison indicates that there is stronger positive vorticity advection, larger inward eddy mode and outward mean mode vorticity transport at the initial and subsequent times. Averaged over 6° latitude (Table 13), the positive vorticity advection is still significantly stronger for the explosive storms. There are consistent differences in the 6° radius eddy and mean mode of vorticity transport, but not to the degree that allows statistical separation.

Figs. 10 through 12 show that over a 24 h period, the vorticity advection has large positive values that vary with time for both storms groups. Specifically, the maximum positive vorticity advection was at the 12 h point. The initially strong positive vorticity advection became more intense during the first 12 h, presumably through the self-development process (Petterssen, 1956). This self-development process is the strengthening of the upper-level wave that results in greater cold advection to the west and greater warm advection to the east. The increase in warm and cold advection act to intensify the positive vorticity advection. In the explosive cases, the continuation of cyclogenesis after 12 h results in a vertically developed system. The slight decrease in magnitude of the values after the 12 h indicates a lessening in the deepening rate of the storms.

The eddy and mean mode values are in agreement with the previous discussion of the vorticity advection, and peak at the 12 h mark as shown in Figs. 13 and 17 (where the inward eddy mode has positive values and the outward mean mode has negative values). The eddy mode of vorticity transport is strongly related to the average positive vorticity advection (PVA) term and its agreement with the PVA term reinforces the importance of strong upper-level influences on explosive cyclogenesis. The mean mode of vorticity transport isolates the role of the upper-level divergence in the cyclone's vorticity budget. The stronger negative mean mode results documents stronger divergence aloft for the explosive cyclogenesis set in agreement with the vertical motion results presented above.

The upper-level divergence, as estimated by the outward mass transport values, has similar fluctuations with significantly larger values for the explosive cases (up to a factor of four) compared to the nonexplosive ones (Figs. 19 to 21). The divergence term showed the greatest variability of all the upper-level properties, particularly for the explosive systems. The primary reason for this variability was probably the difficulty in analyzing the tropospheric winds.

The upper-level forcing terms for explosive and nonexplosive storms contained statistical separation in over half of the categories. The largest separation is at the storm onset where the explosive storms had three times the divergence of the nonexplosive ones at the 4° radius. The differences between the explosive and nonexplosive cases gradually decreased to 50 percent as the deepening progressed. The best separation between the explosive and nonexplosive sets of storms for the upper-troposphere parameters was at the 4° radius. This suggests the important upper-tropospheric features are near the surface cyclone center and not spread over a large area.

G. TWENTY-FOUR HOUR AVERAGE STORM COMPARISON

The 24-h averaged values used to describe cyclone development are listed in Tables 14 through 18. The overall strength of the low-level baroclinic, low-level circulation and upper-level forcing for the explosive and nonexplosive cyclones can be compared in these tables. Table 14 shows the sea-level pressure for both types of storms. The sea-level pressure average for 24-h average was 18 mb greater for the explosive cases compared to the nonexplosive cases.

The low-level baroclinic structure of the explosive and nonexplosive storms were very similar with the exception of the former having a higher area-averaged potential temperature by 4° (for the 4° and 6° latitude radius). The static stability values were less

(Table 15) for the explosive storms by a margin of approximately 0.5 degrees, which was not statistically significant.

The computed kinematic vertical velocities in Table 16 were consistent with the observed upper-level parameters. The explosive cyclones have consistently stronger upward motion at the 700 and 850 mb levels. The absolute vorticity averaged for 24 h showed higher values at the 4° radius compared to the 6° radius position, even though the initial values were higher for the nonexplosive cyclones (Table 17). However, as time progressed, the explosive storms gained intensity and eventually showed a sizeable increase over the nonexplosive storms.

The upper-level diagnostic terms averaged over a 24 h period (Table 18), indicate that there was a significant amount of of upper-level forcing in the explosive cyclogenesis development The vorticity advection was positive in all cases with the explosive storms having nearly double the values of the nonexplosive cases (Table 18). The upper-level divergence was approximately two to three times larger for the explosive storms (however, the amount varied with time).

H. SUMMARY

The key result of this chapter is that the kinematic vertical velocity and the upper-level forcing mechanisms are statistically separable. The large values for the upper-level processes suggests that the upper-tropospheric wave influence is most likely to produce the stronger vertical motions that accompany explosive cyclogenesis. In contrast, the low-level baroclinity and static stability did not show a statistical separation, which indicates that the explosive and nonexplosive storms share a similar low-level frontal strength in a weak static stability environment. The statistical separation of the explosive and nonexplosive cyclones is stronger than in the early results of Smith (1986). The reasons for their improvement likely stem from the revised FGGE analyses as well as a better delineation of the storm tracks and intensity.

The evolution of the upper-level developmental parameters is characterized by maximum values occurring at 12 h in the middle of the explosive deepening period. At this decisive point, the storm either continued to develop as in the explosive cases or starts to weaken. However, the low-level circulation continues to increase to 24 h and does not reach a peak value after 12 h. In addition, the static stability continues to decrease but at a lesser rate during the last 12 h.

In the next chapter these events are explored and evaluated. The conclusions are discussed and recommendations were offered in an effort to gain insight on the important mechanisms of explosive cyclogenesis.

Table 7. TWENTY-FOUR HOUR TIME EVOLUTION OF LOW-LEVEL ABSOLUTE VORTICITY FOR BOTH STORM GROUPS (4° AND 6° RADII). Standard deviations are listed in parentheses and 't' subscript indicates explosive and nonexplosive sets are statistically different at a 10% significance level.

SIZE	RADIUS 4°		RADIUS 6 °	
ABSOLUTE VORTICITY(10E-6/S)	EX-PLOSIVE	NON-EXP	EX-PLOSIVE	NON-EXP
1000 - 850 MB	(10E-6/SEC)	(10E-6/SEC)	(10E-6/SEC)	(10E-6/SEC)
T = 0 h	118 (17)	130 (23)	101 (17)	114 (22)
T = 12 h	149 (19)	145 (26)	117 (17)	120 (18)
T = 24 h	174_t (19)	153_t (24)	130 (16)	129 (21)

Table 8. **TWENTY-FOUR HOUR EVOLUTION OF KINEMATIC VERTICAL MOTION FOR BOTH STORM GROUPS (4° RADIUS).** Standard deviations are listed in parentheses and 't' subscript indicates explosive and nonexplosive sets are statistically different at a 10% significance level.

DESCRIPTION	EXPLOSIVE	NONEX-PLOSIVE
OMEGA 850 MB	(10E-4MB/SEC)	(10E-4MB/SEC)
T = 0 h	-206_t (143)	-106_t (83)
T = 12 h	−175 (138)	−118 (152)
T = 24 h	-167_t (109)	-85_t (70)
700 MB	(10E-4MB/SEC)	(10E-4MB/SEC)
T = 0 h	-180_t (119)	-69_t (95)
T = 12 h	−155 (119)	−100 (128)
T = 24 h	-132_t (68)	-68_t (92)

Table 9. **TWENTY-FOUR HOUR EVOLUTION OF KINEMATIC VERTICAL MOTION FOR BOTH STORM GROUPS (6° RADIUS).** Standard deviations are listed in parentheses and 't' subscript indicates explosive and nonexplosive sets are statistically different at a 10% significance level.

DESCRIPTION	EXPLOSIVE	NONEX-PLOSIVE
OMEGA 850 MB	(10E-4MB/SEC)	(10E-4MB/SEC)
T = 0 h	-156_t (97)	-95_t (81)
T = 12 h	-165_t (109)	-101_t (70)
T = 24 h	-127_t (72)	-91_t (69)
700 MB	(10E-4MB/SEC)	(10E-4MB/SEC)
T = 0 h	-134_t (82)	-71_t (74)
T = 12 h	-146_t (93)	-84_t (60)
T = 24 h	−111 (63)	−68 (91)

Table 10. **TWENTY-FOUR HOUR TIME EVOLUTION OF THERMAL STRUCTURE FOR BOTH STORM GROUPS (4° RADIUS).** Standard deviations are listed in parentheses and 't' subscript indicates explosive and nonexplosive sets are statistically different at a 10% significance level.

DESCRIPTION	EXPLOSIVE	NONEX-PLOSIVE
STATIC STABILITY ($d\theta/dP$) 1000-500 MB	(° K/100 MB)	(° K/100 MB)
T = 0 h	−4.70 (1.26)	−5.20 (1.46)
T = 12 h	−4.45 (0.83)	−4.91 (0.88)
T = 24 h	−4.41 (0.66)	−4.61 (0.88)
FRONTAL ZONE THERMAL STRENGTH	Δ T	Δ T
1000-500 MB	° K	° K
T = 0 h	15 (3.33)	14 (3.66)
T = 12 h	16 (3.43)	13 (4.56)
T = 24 h	14 (4.39)	13 (5.31)
1000-800 MB	° K	° K
T = 0 h	17 (4.32)	15 (3.81)
T = 12 h	18 (4.39)	16 (4.57)
T = 24 h	15 (3.99)	15 (5.85)

Table 11. **TWENTY-FOUR HOUR TIME EVOLUTION OF THERMAL STRUCTURE FOR BOTH STORM GROUPS (6° RADIUS).** Standard deviations are listed in parentheses and 't' subscript indicates explosive and nonexplosive sets are statistically different at a 10% significance level.

DESCRIPTION	EXPLOSIVE	NONEX-PLOSIVE
STATIC STABILITY ($d\theta/dP$) 1000-500 MB	(° K/100 MB)	(° K/100 MB)
T = 0 h	−4.86 (1.19)	−5.27 (1.22)
T = 12 h	-4.54_t (0.72)	-5.10_t (0.88)
T = 24 h	−4.50 (0.61)	−4.86 (0.84)
FRONTAL ZONE THERMAL STRENGTH	Δ T	Δ T
1000-500 MB	° K	° K
T = 0 h	20 (3.45)	19 (4.78)
T = 12 h	20 (4.38)	19 (6.21)
T = 24 h	18 (3.83)	18 (5.99)
1000-800 MB	° K	° K
T = 0 h	24_t (5.60)	20_t (5.15)
T = 12 h	23 (5.89)	22 (7.5)
T = 24 h	21 (3.6)	22 (7.23)

Table 12. TWENTY-FOUR HOUR EVOLUTION OF UPPER-LEVEL PROPERTIES AVERAGED FROM 500 TO 200 MB (4° RADIUS). Standard deviations are listed in parentheses and 't' subscript indicates explosive and nonexplosive sets are statistically different at a 10% significance level.

DESCRIPTION	EXPLOSIVE	NONEXPLOSIVE
VORTICITY ADVECTION	(10E-11/SEC2)	(10E-11/SEC2)
T = 0 h	163_t (89)	72_t (84)
T = 12 h	177_t (118)	79_t (61)
T = 24 h	92_t (55)	61_t (35)
EDDY MODE OF VORTICITY TSPT	(10E-11/SEC2)	(10E-11/SEC2)
T = 0 h	136_t (93)	72_t (91)
T = 12 h	182_t (115)	87_t (99)
T = 24 h	80_t (80)	35_t (50)
MEAN MODE OF VORTICITY TSPT	(10E-11/SEC2)	(10E-11/SEC2)
T = 0 h	-81_t (39)	-53_t (32)
T = 12 h	-81_t (59)	-46_t (36)
T = 24 h	-70_t (57)	-35_t (15)
UPPER-LEVEL DIVERGENCE	(10E-10 GM/SEC)	(10E-10 GM/SEC)
T = 0 h	250 (319)	157 (103)
T = 12 h	442 (326)	152 (125)
T = 24 h	264 (223)	85 (71)

Table 13. **TWENTY-FOUR HOUR EVOLUTION OF UPPER-LEVEL PROPERTIES AVERAGED FROM 500 TO 200 MB (6° RADIUS).** Standard deviations are listed in parentheses and 't' subscript indicates explosive and nonexplosive sets are statistically different at a 10% significance level.

DESCRIPTION	EXPLOSIVE	NONEXPLOSIVE
VORTICITY ADVECTION	(10E-11/SEC2)	(10E-11/SEC2)
T = 0 h	101_t (60)	60_t (39)
T = 12 h	105_t (55)	55_t (35)
T = 24 h	92 (91)	52 (31)
EDDY MODE OF VORTICITY TSPT	(10E-11/SEC2)	(10E-11/SEC2)
T = 0 h	79 (59)	60 (65)
T = 12 h	118 (68)	84 (55)
T = 24 h	61 (58)	44 (35)
MEAN MODE OF VORTICITY TSPT	(10E-11/SEC2)	(10E-11/SEC2)
T = 0 h	−49 (22)	−40 (19)
T = 12 h	-63_t (26)	-34_t (26)
T = 24 h	-56_t (29)	-33_t (16)
UPPER-LEVEL DIVERGENCE	(10E-10 GM/SEC)	(10E-10 GM/SEC)
T = 0 h	372 (666)	305 (141)
T = 12 h	825_t (685)	181_t (139)
T = 24 h	342 (380)	181 (144)

Table 14. TWENTY-FOUR HOUR AVERAGE OF SEA-LEVEL PRESSURE FOR BOTH STORM GROUPS (4° AND 6° RADII).

DESCRIPTION	EXPLOSIVE	NONEX-PLOSIVE
STORM TYPE	PRESSURE	PRESSURE
Initial Surface Pressure (MB)	1006	1006
24 H Surface Pressure Change (MB)	28	10

Table 15. TWENTY-FOUR HOUR AVERAGE THERMAL STRUCTURE FOR BOTH STORM GROUPS (4° AND 6° RADII).

SIZE	RADIUS 4 °		RADIUS 6 °	
STATIC STABILITY ($d\theta/dP$)(° K/100MB)	EX-PLOSIVE	NON-EXP	EX-PLOSIVE	NON-EXP
1000-500 MB	-4.52	-4.91	-4.63	-5.07
FRONTAL ZONE THERMAL STRENGTH (ΔT)	° K	° K	° K	° K
1000 - 500 MB	15	14	19	19
1000 - 800 MB	17	15	23	21

Table 16. TWENTY-FOUR HOUR AVERAGE KINEMATIC VERTICAL MOTION FOR BOTH STORM GROUPS (4° AND 6° RADII).

SIZE	RADIUS 4 °		RADIUS 6 °	
DESCRIPTION	EX-PLOSIVE	NON-EXP	EX-PLOSIVE	NON-EXP
OMEGA	(10E-4MB S)	(10E-4MB S)	(10E-4MB S)	(10E-4MB S)
850 MB	160	96	117	106
700 MB	121	104	102	95

Table 17. TWENTY-FOUR HOUR AVERAGE OF LOW-LEVEL ABSOLUTE VORTICITY FOR BOTH STORM GROUPS (4° AND 6° RADII).

SIZE	RADIUS 4°		RADIUS 6 °	
DESCRIPTION	EX-PLOSIVE	NON-EXP	EX-PLOSIVE	NON-EXP
ABSOLUTE VORTICITY	(10E-6/SEC)	(10E-6/SEC)	(10E-6/SEC)	(10E-6/SEC)
1000-850 MB	147	142	116	121

Table 18. TWENTY-FOUR HOUR AVERAGE UPPER-LEVEL FORCING PROPERTIES FOR BOTH STORM GROUPS (500-200 MB AT 4° AND 6° RADII).

SIZE	RADIUS 4 °		RADIUS 6 °	
DESCRIPTION	EX-PLOSIVE	NON-EXP	EX-PLOSIVE	NON-EXP
VORTICITY ADVECTION (10E-11/SEC2)	144	70	101	58
EDDY MODE (10E-11/SEC2)	133	75	86	63
MEAN MODE (10E-11/SEC2)	-77	-45	-56	-37
UPPER-LEVEL DIVERGENCE(10E-10 GM/SEC)	318	131	512	222

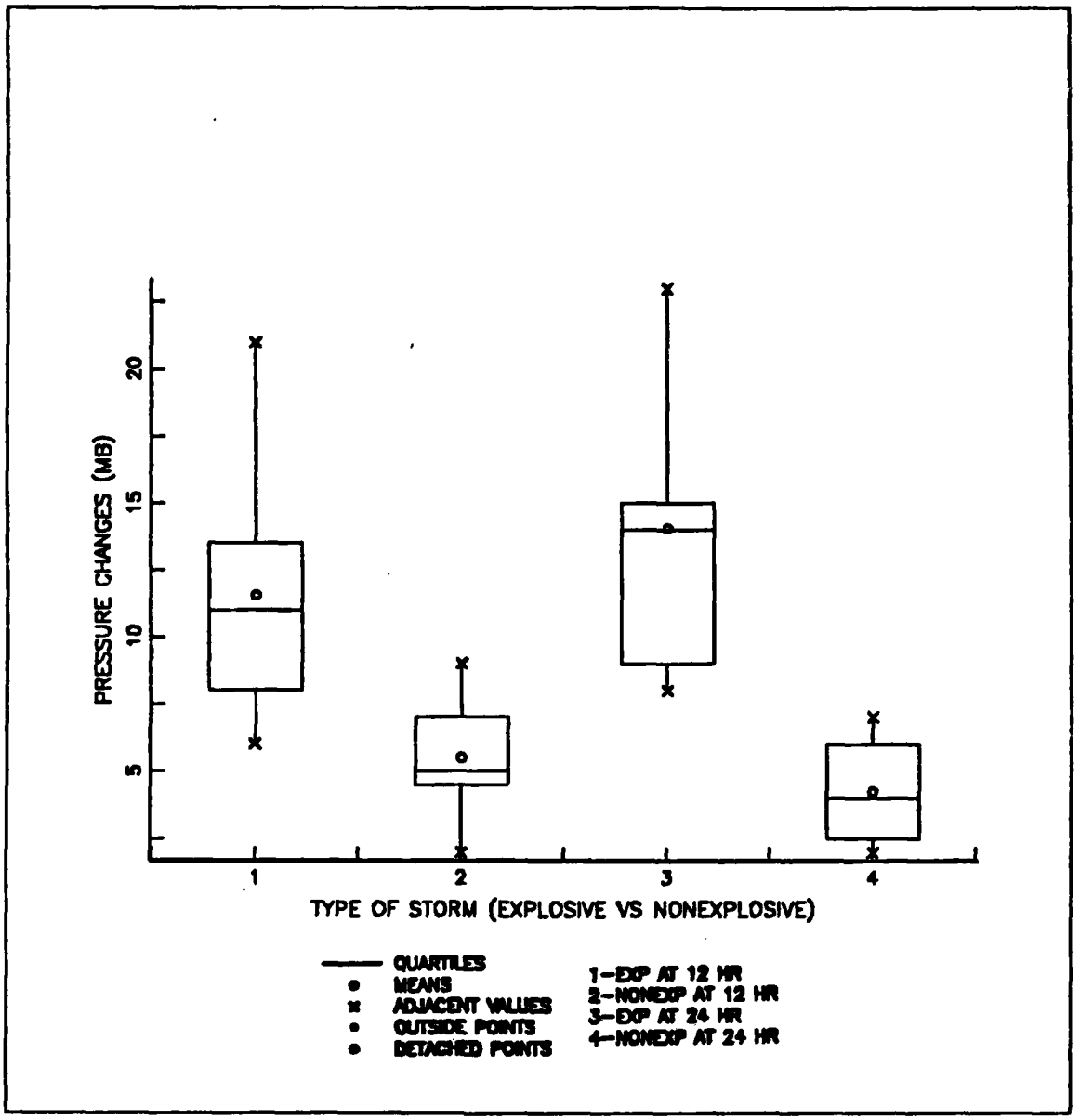

Figure 3. Pressure changes after 12 (inner plot) and 24-h for explosive and nonexplosive storms in box plot format.

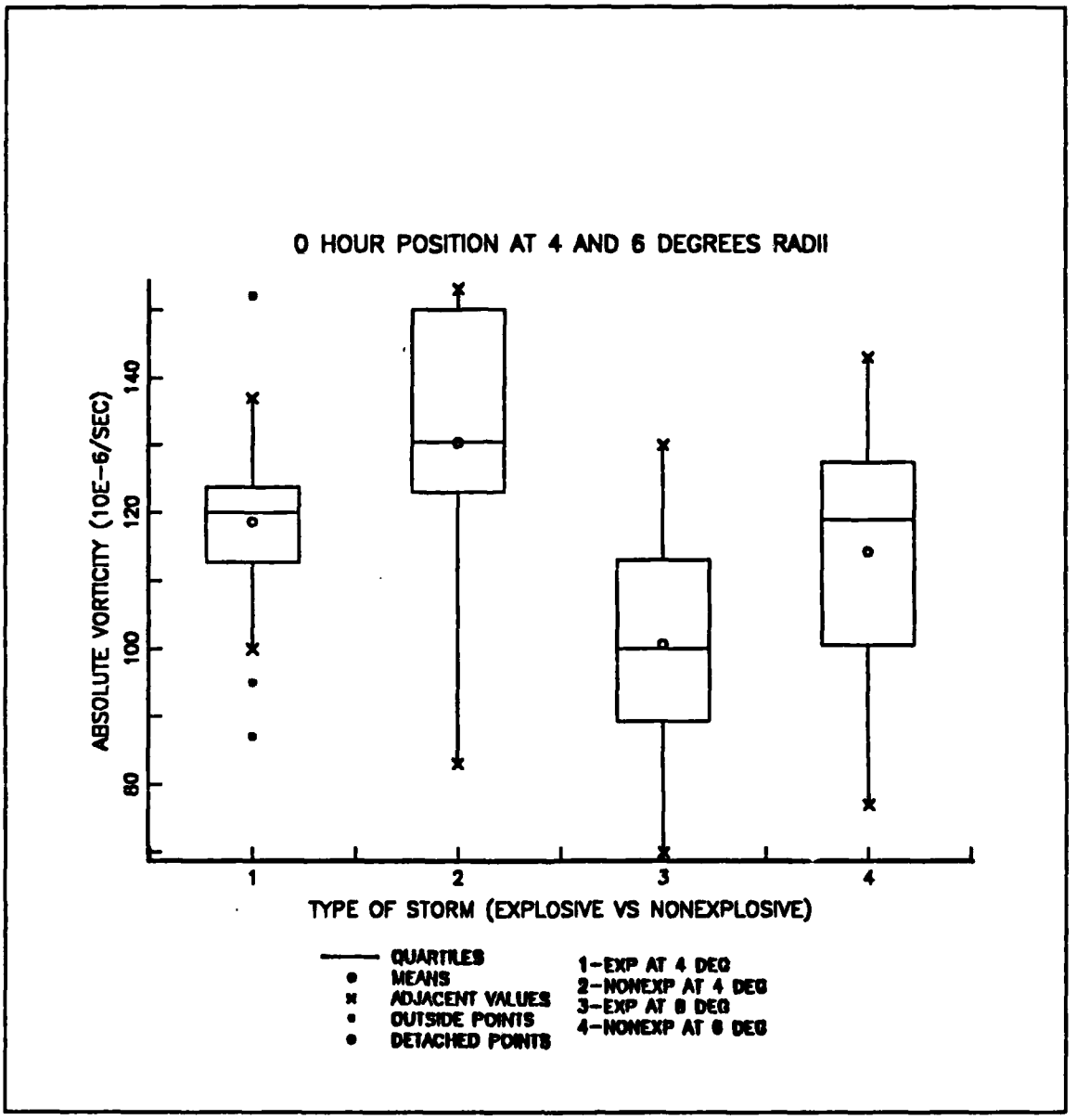

Figure 4. Average absolute vorticity (1000-850 mb) box plots for initial explosive and nonexplosive storms.

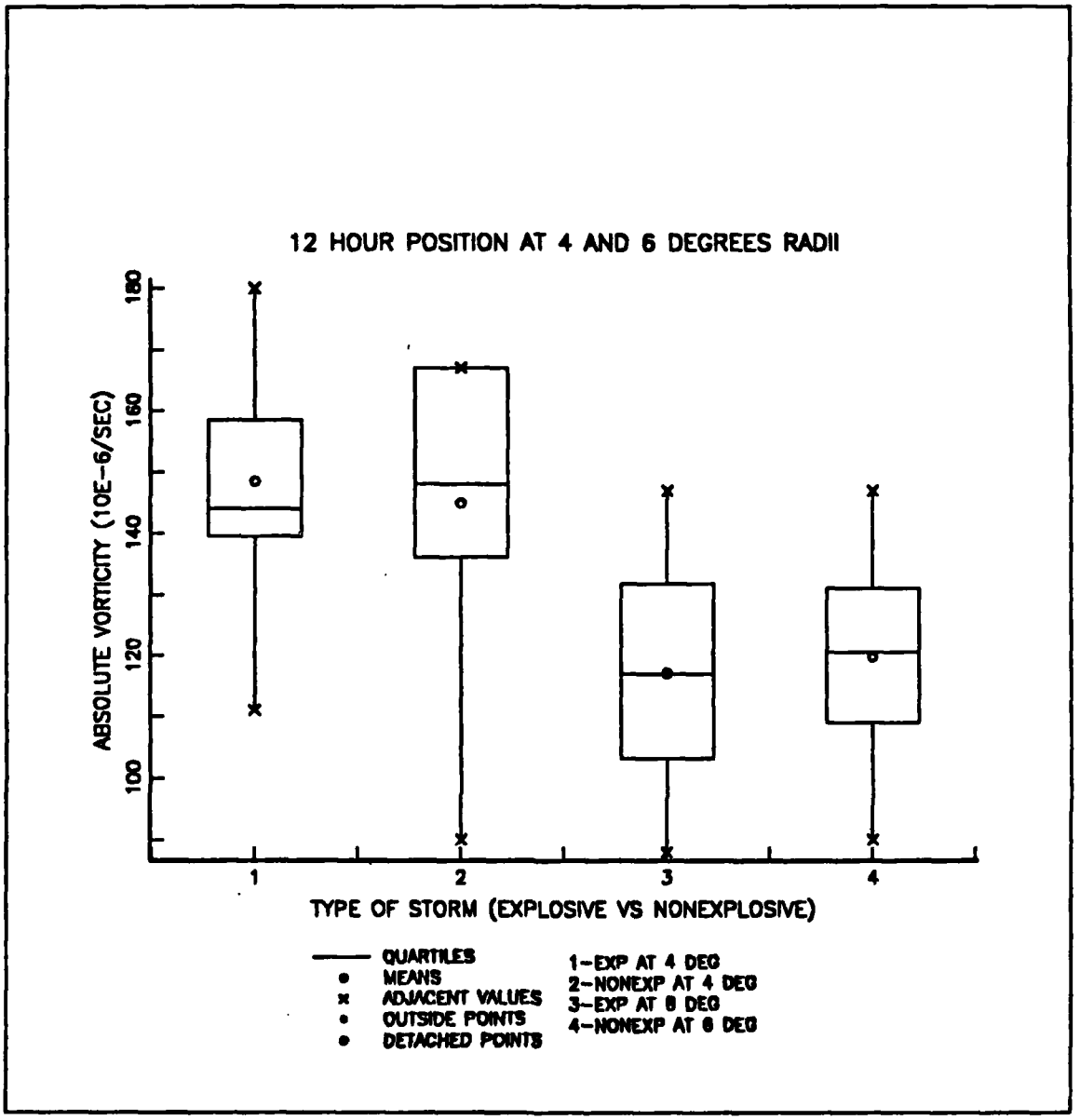

Figure 5. Average absolute vorticity (1000-850 mb) box plots for the 12-h mark.

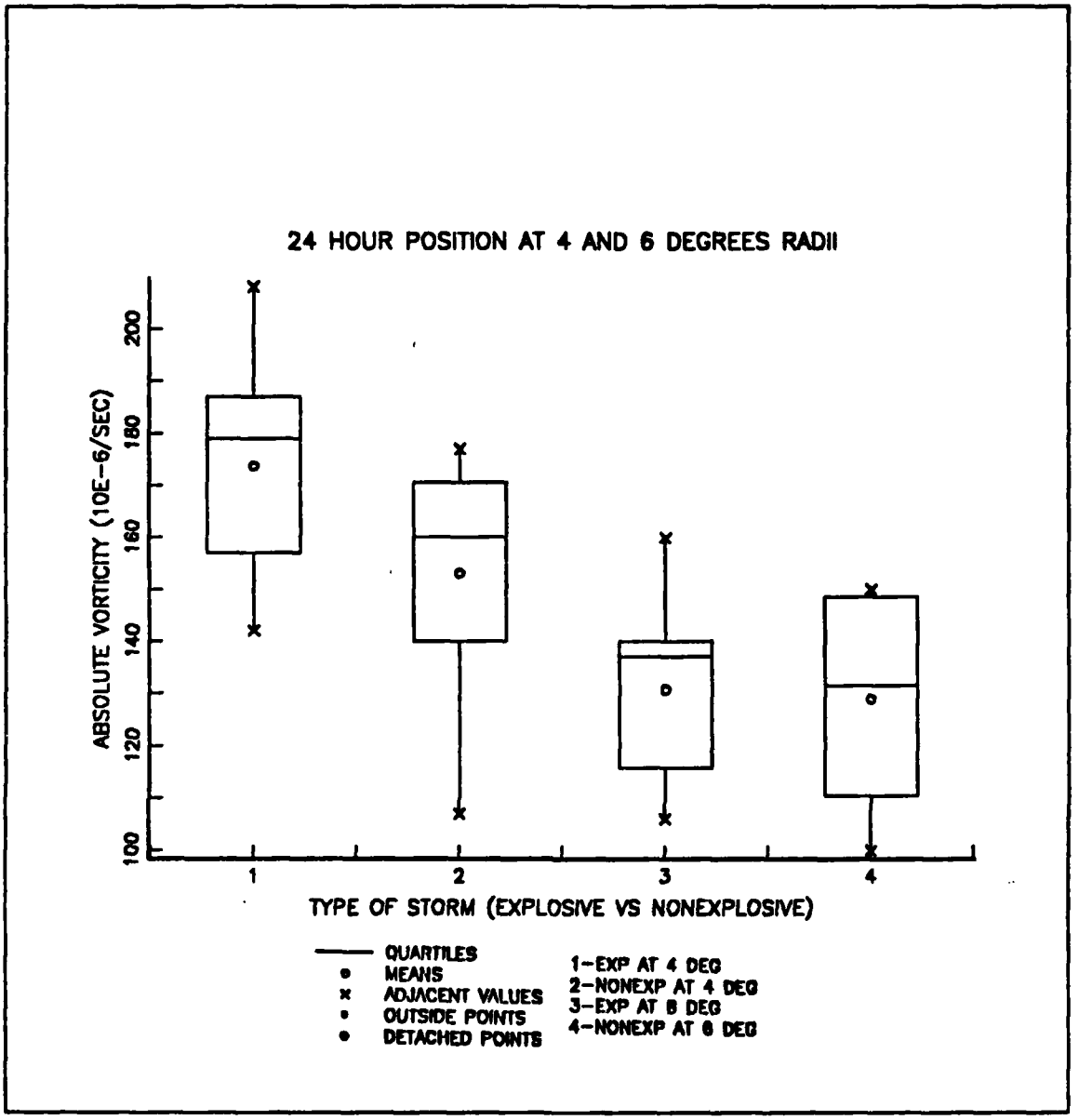

Figure 6. Average absolute vorticity (1000-850 mb) box plots for the 24-h mark.

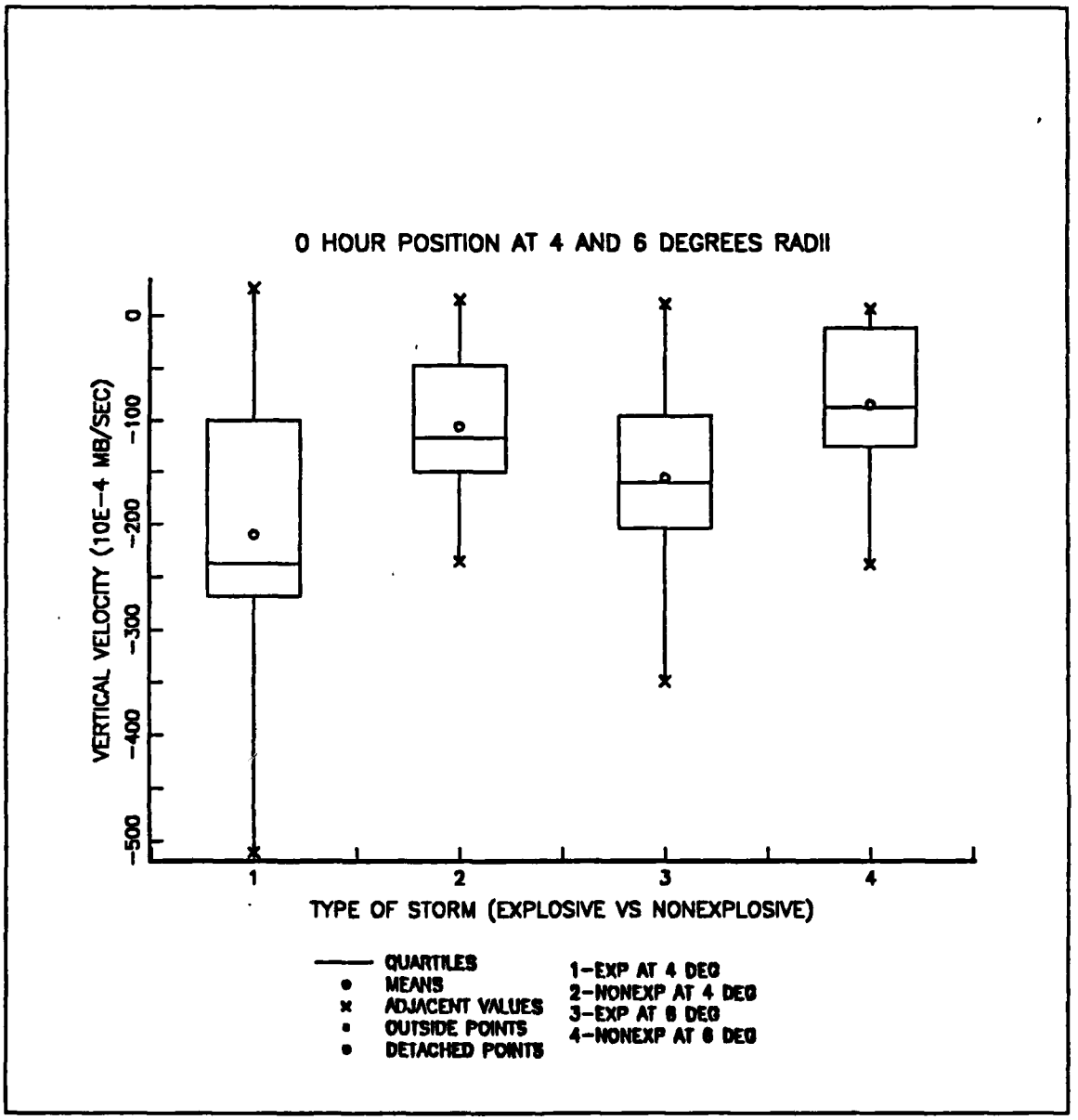

Figure 7. Kinematic vertical velocity (850 mb) box plots for initial explosive and nonexplosive storms.

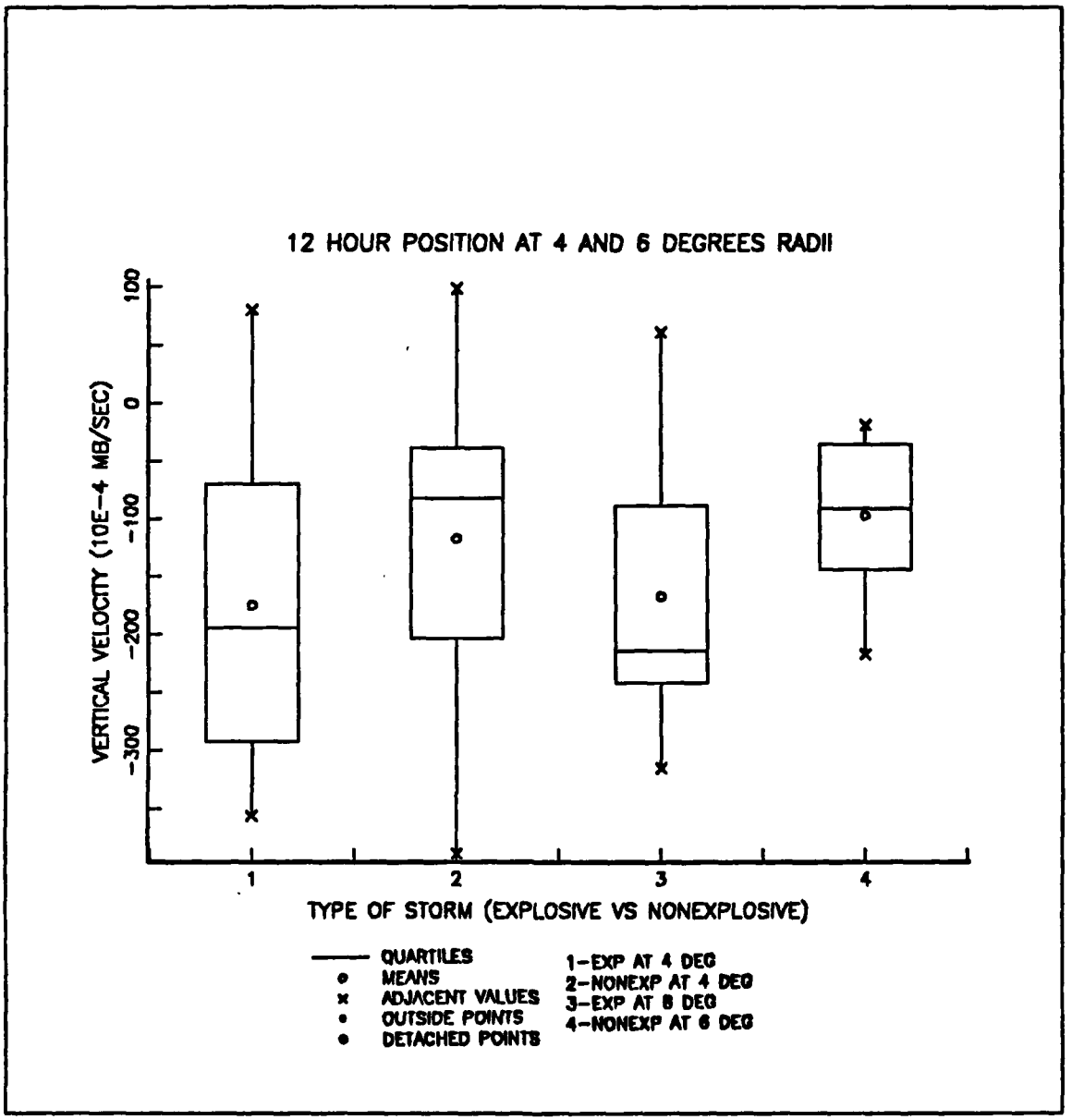

Figure 8. Kinematic vertical velocity (850 mb) box plots for the 12-h mark.

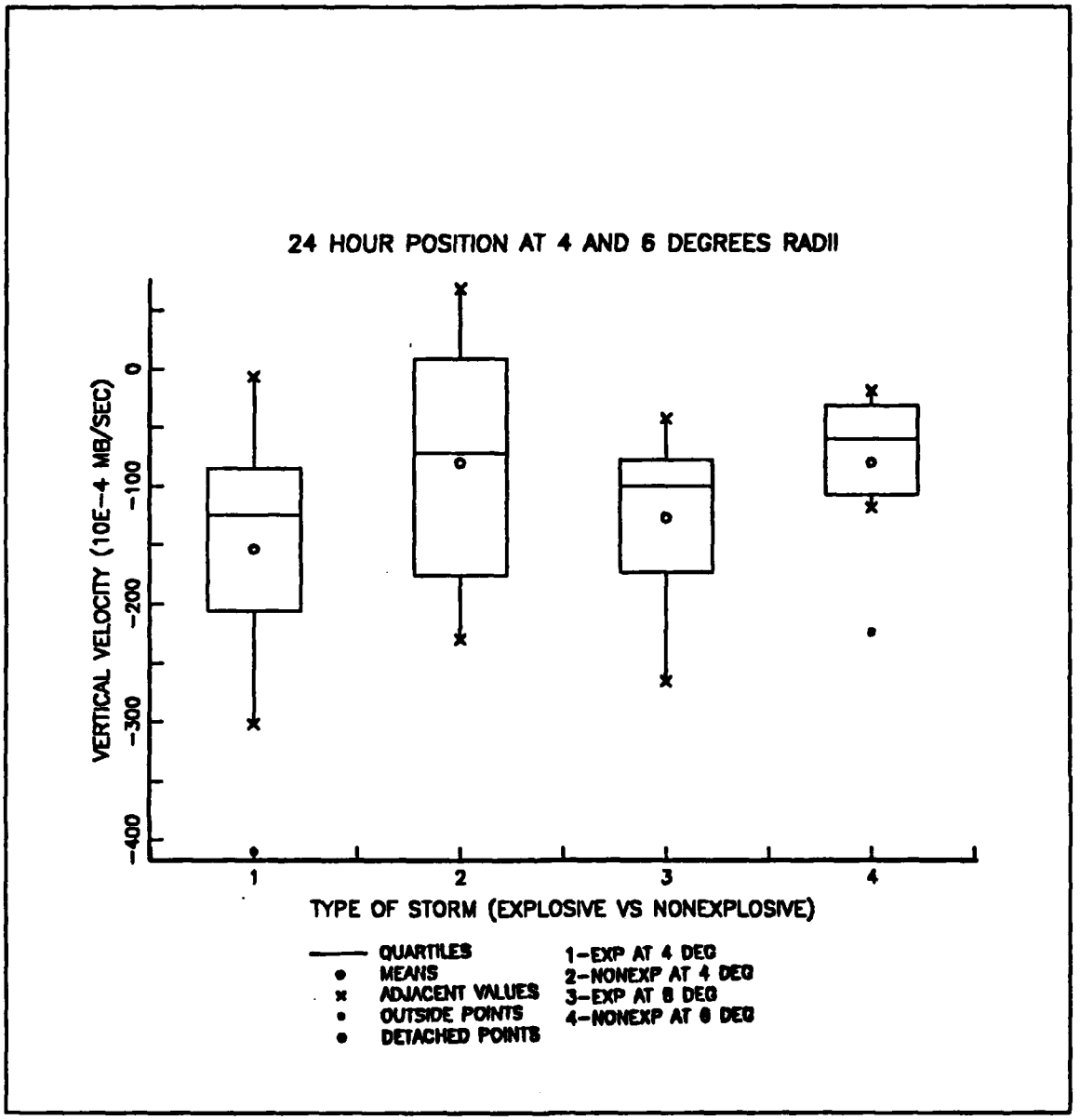

Figure 9. Kinematic vertical velocity (850 mb) box plots for the 24-h mark.

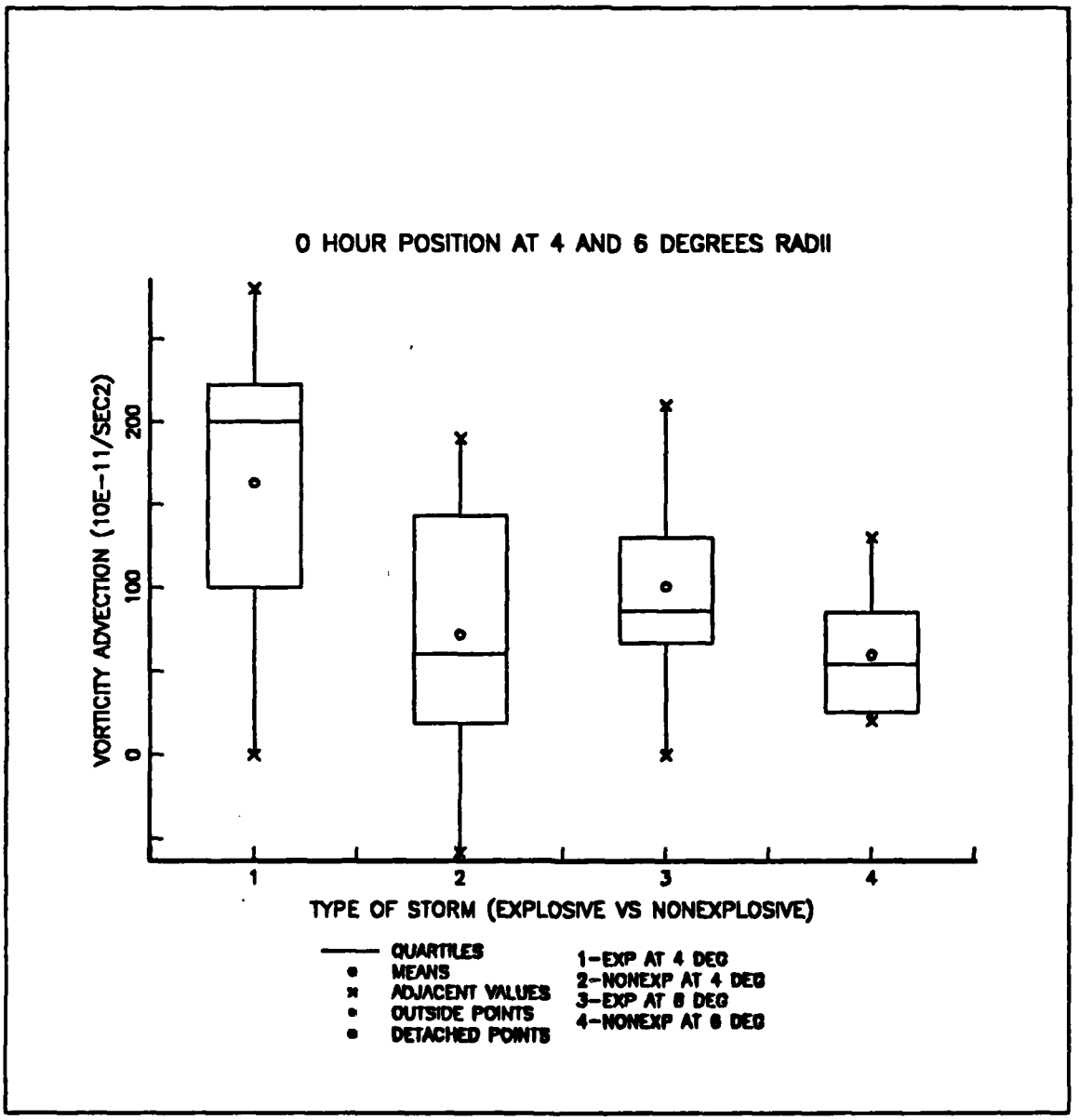

Figure 10. Upper-level vorticity advection (500-200 mb) box plots for initial explosive and nonexplosive storms.

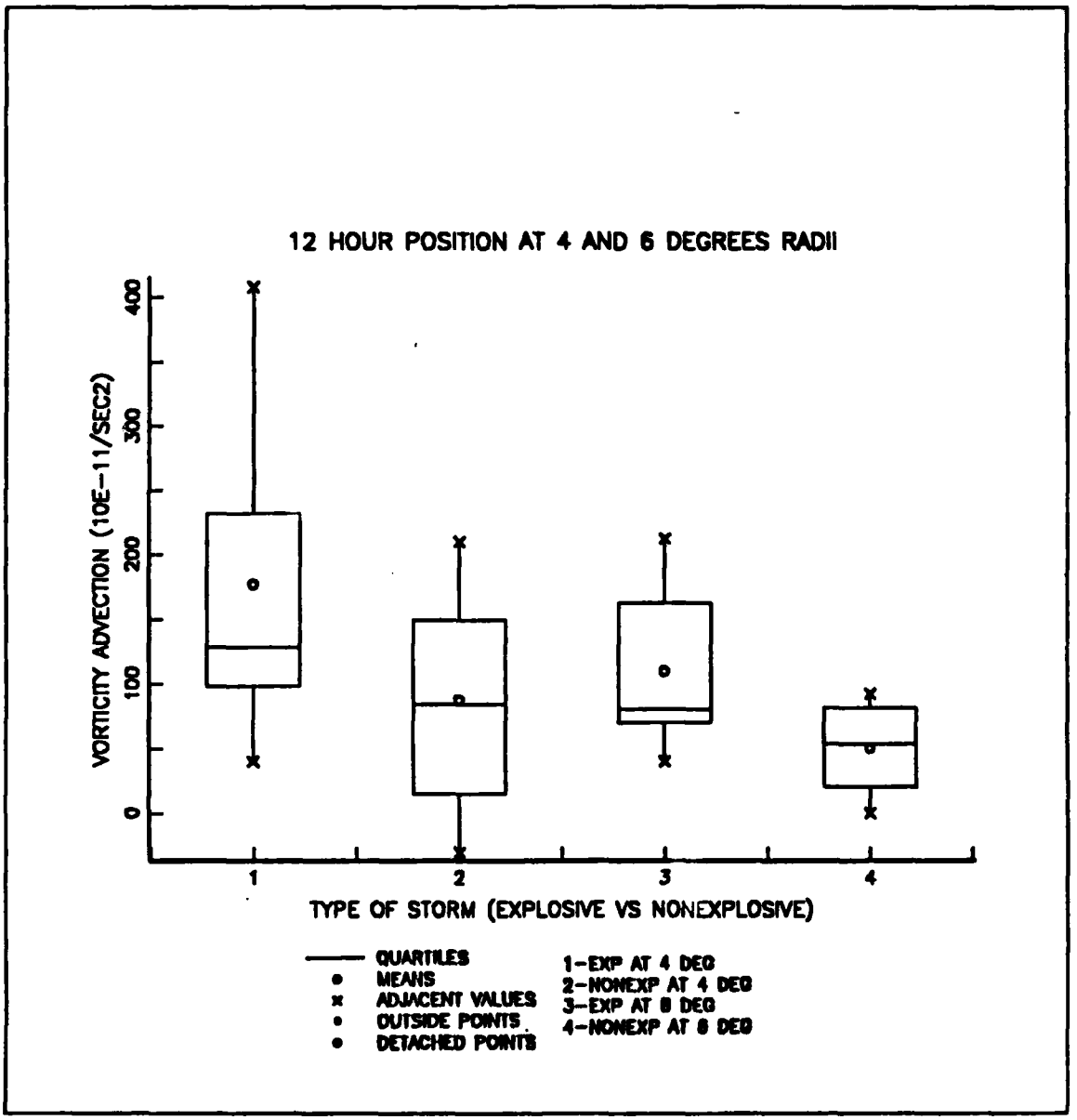

Figure 11. Upper-level vorticity advection (500-200 mb) box plots for the 12-h mark.

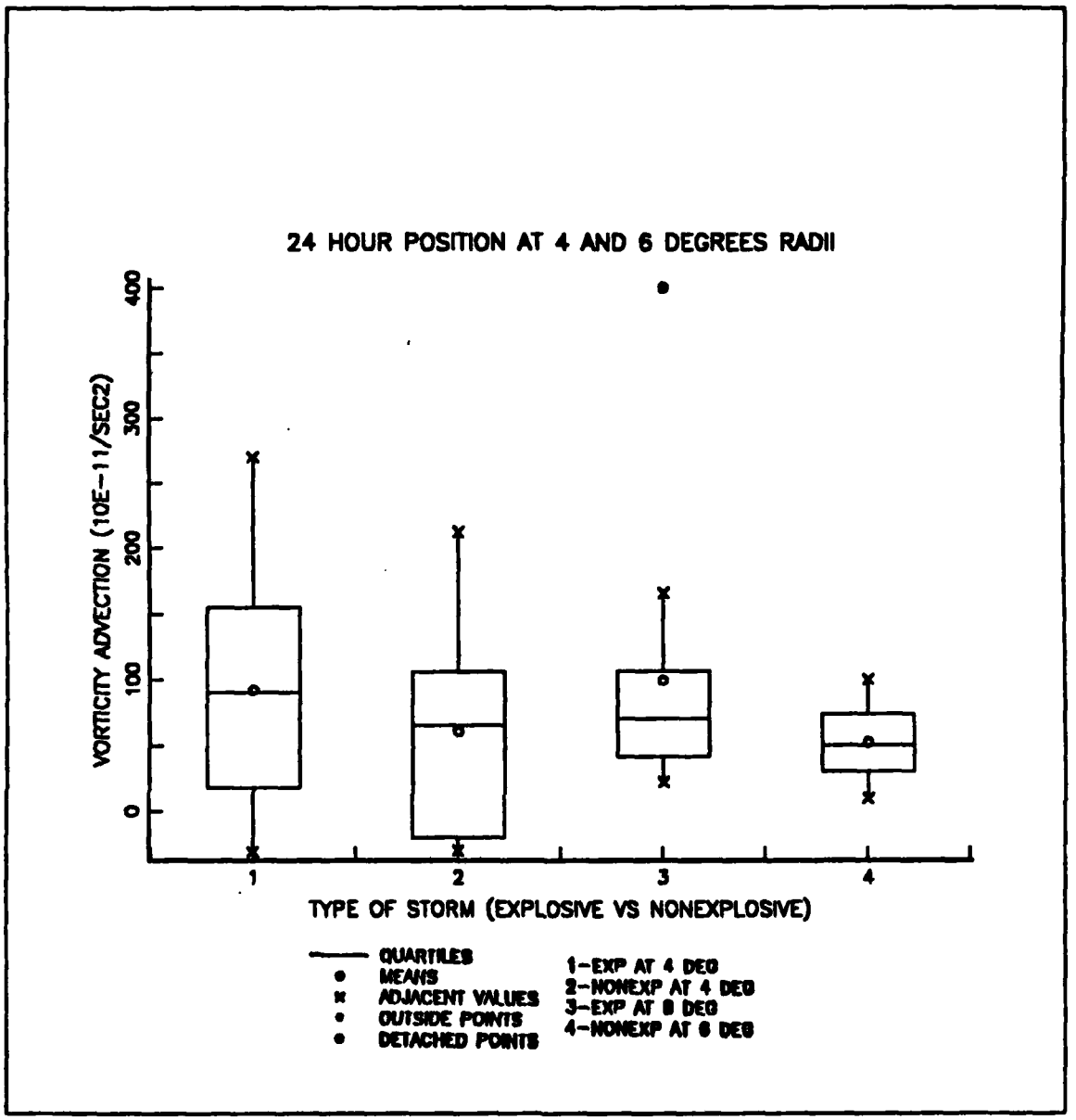

Figure 12. Upper-level vorticity advection (500-200 mb) box plots for the 24-h mark.

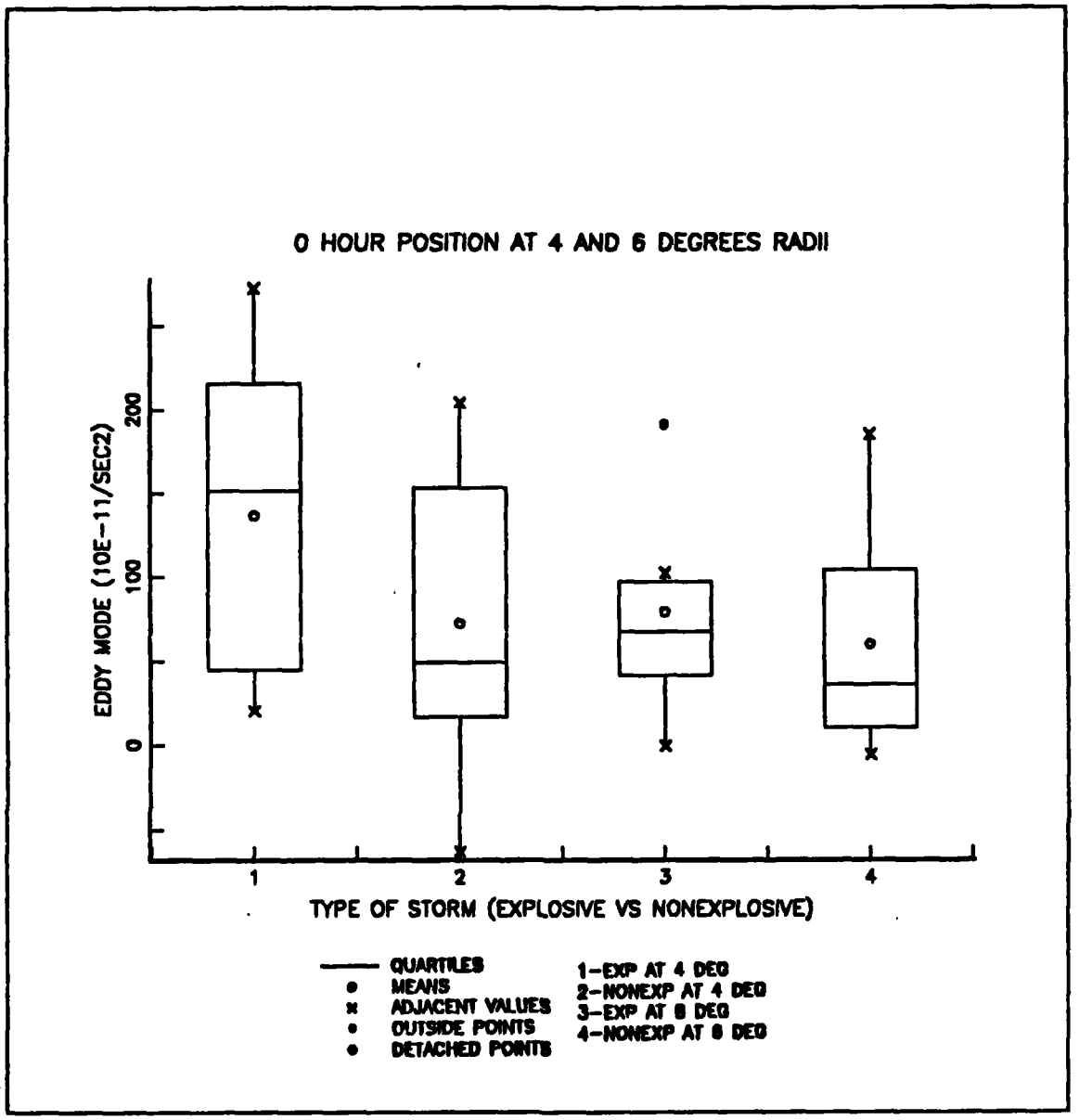

Figure 13. **Averaged eddy mode of vorticity transport (500-200 mb) box plots for initial explosive and nonexplosive storms.**

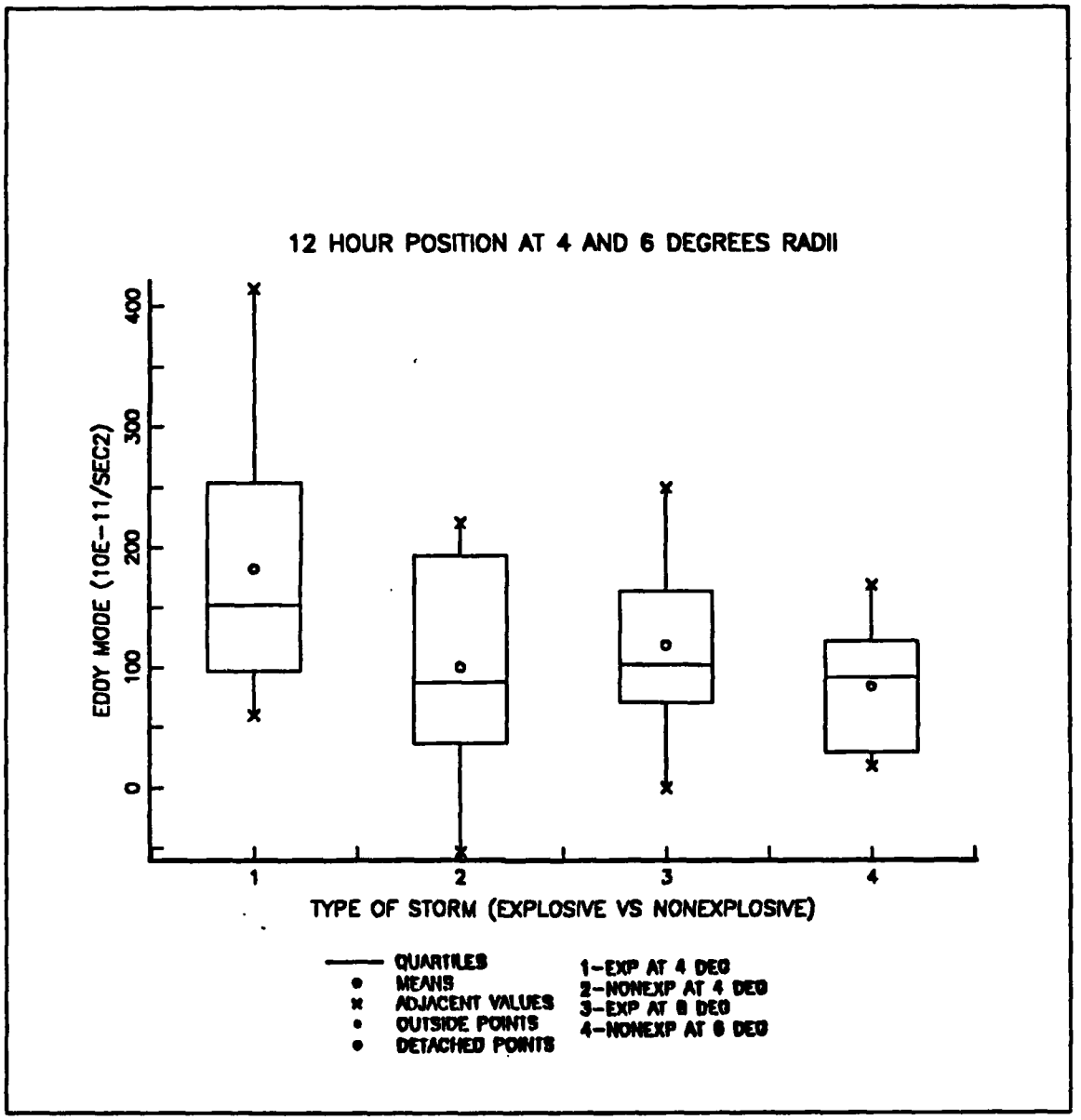

Figure 14. **Averaged eddy mode of vorticity transport (500-200 mb) box plots for the 12-h mark.**

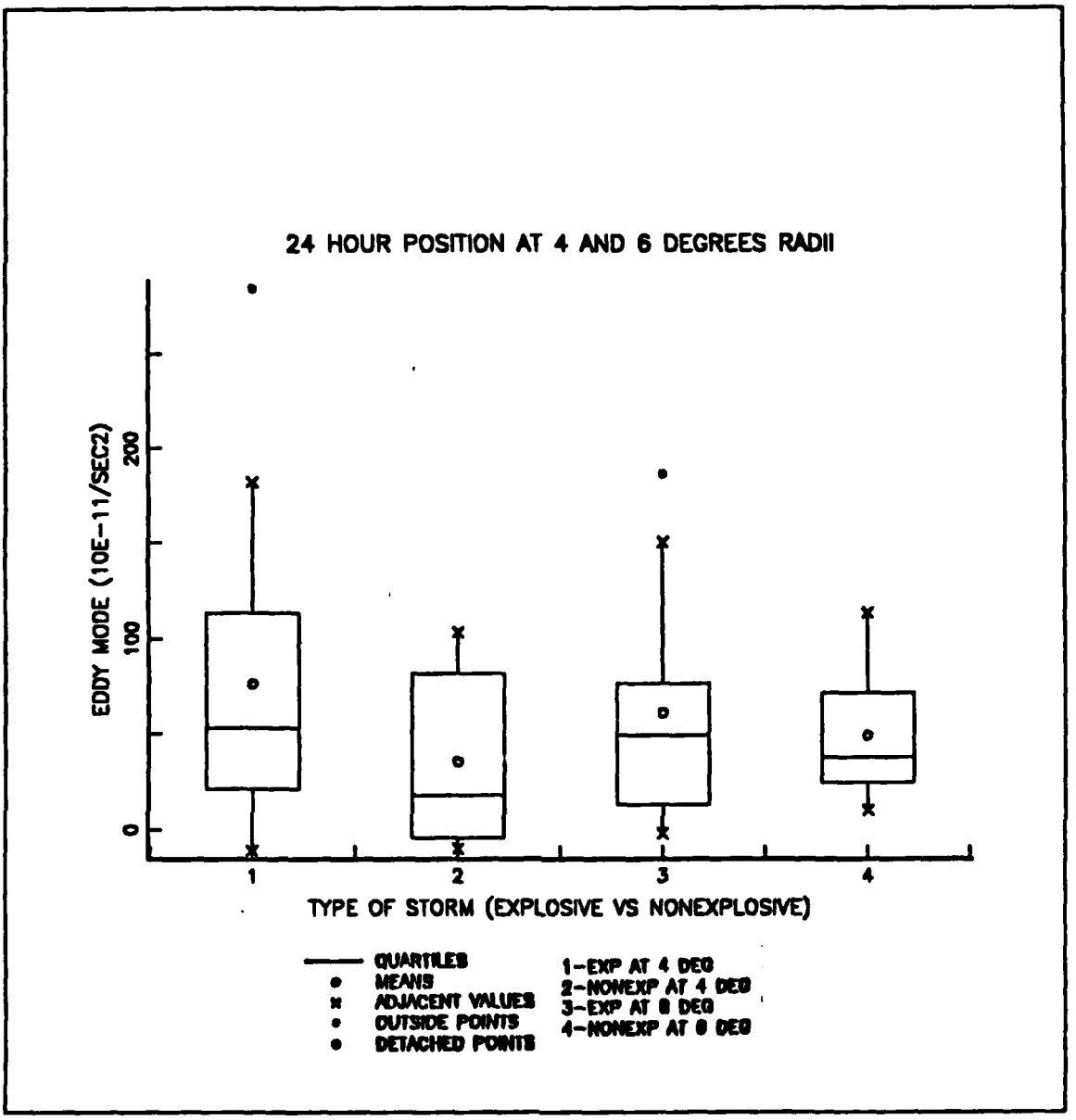

Figure 15. **Averaged eddy mode of vorticity transport (500-200 mb) box plots for the 24-h mark.**

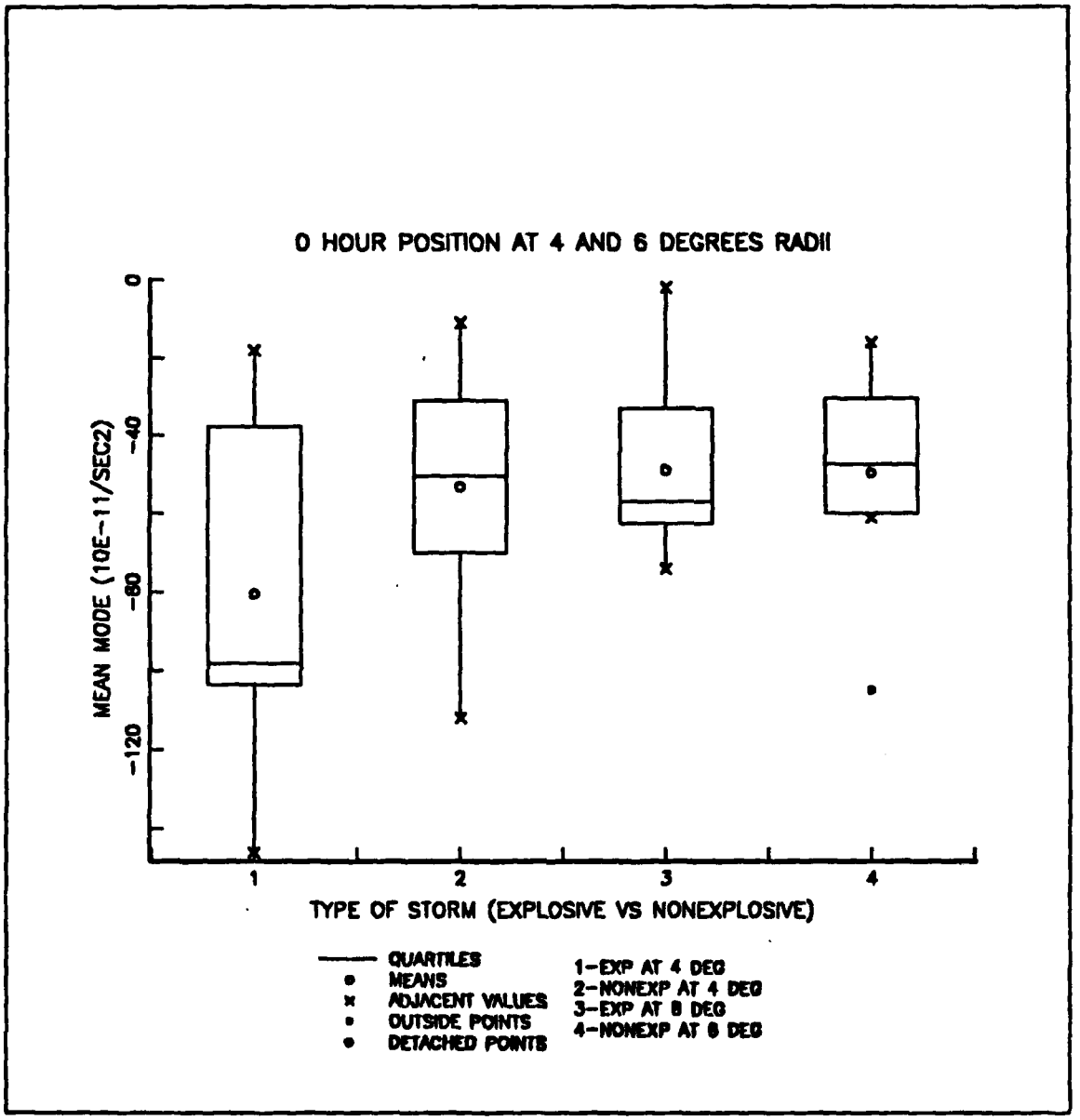

Figure 16. Averaged mean mode of vorticity transport (500-200 mb) box plots for initial explosive and nonexplosive storms.

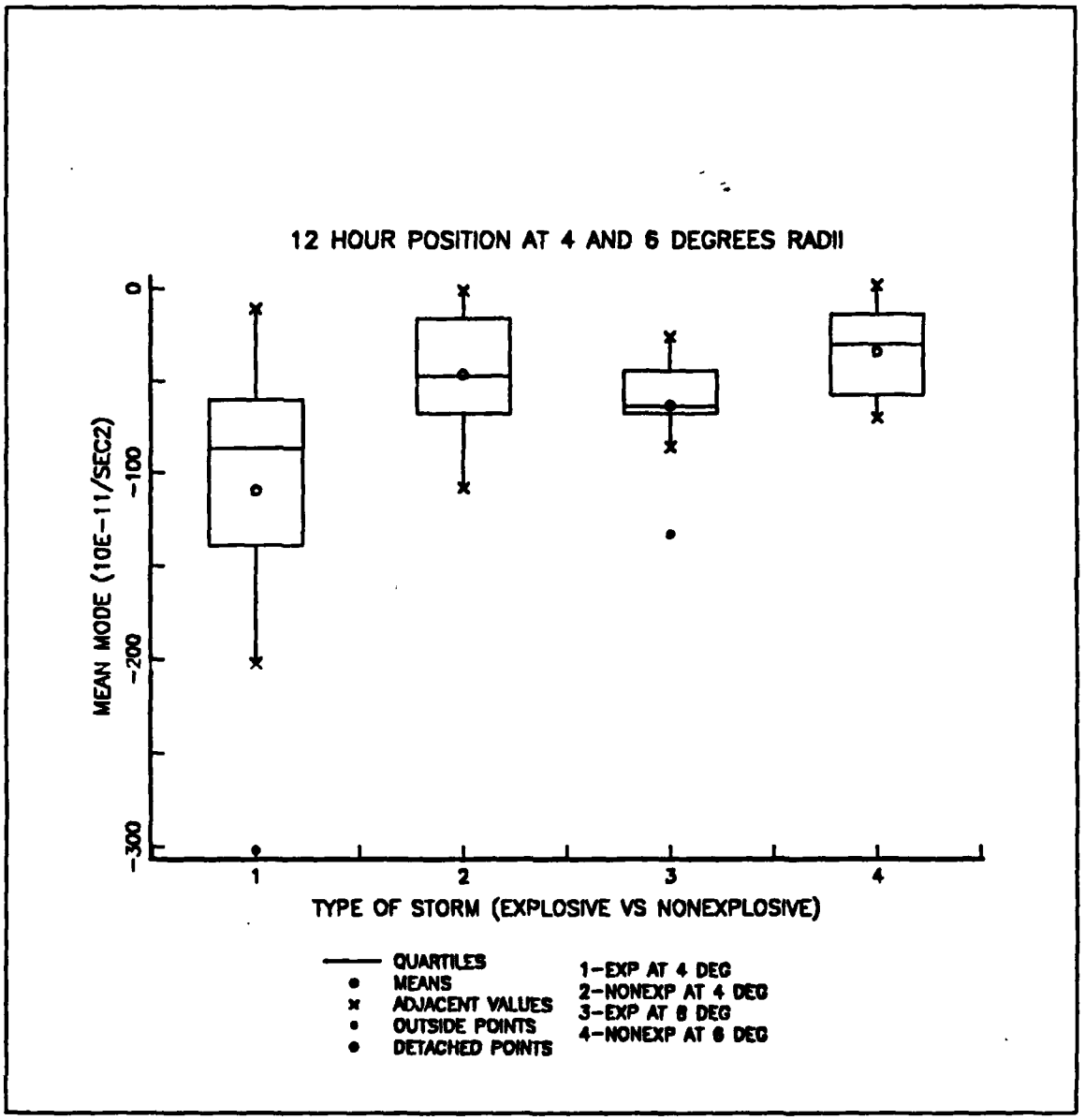

Figure 17. Averaged mean mode of vorticity transport (500-200 mb) box plots for the 12-h mark.

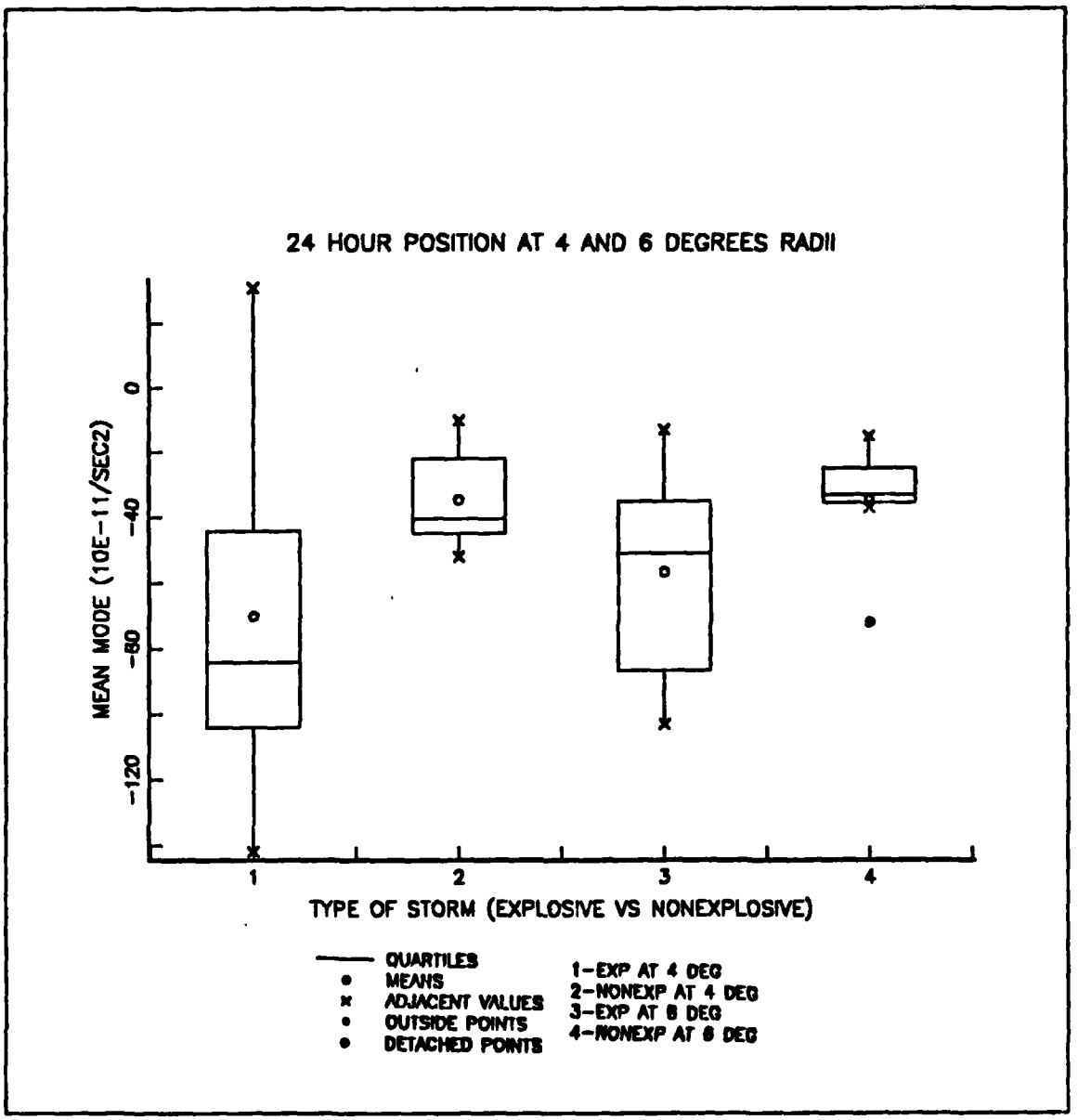

Figure 18. Averaged mean mode of vorticity transport (500-200 mb) box plots for the 24-h mark.

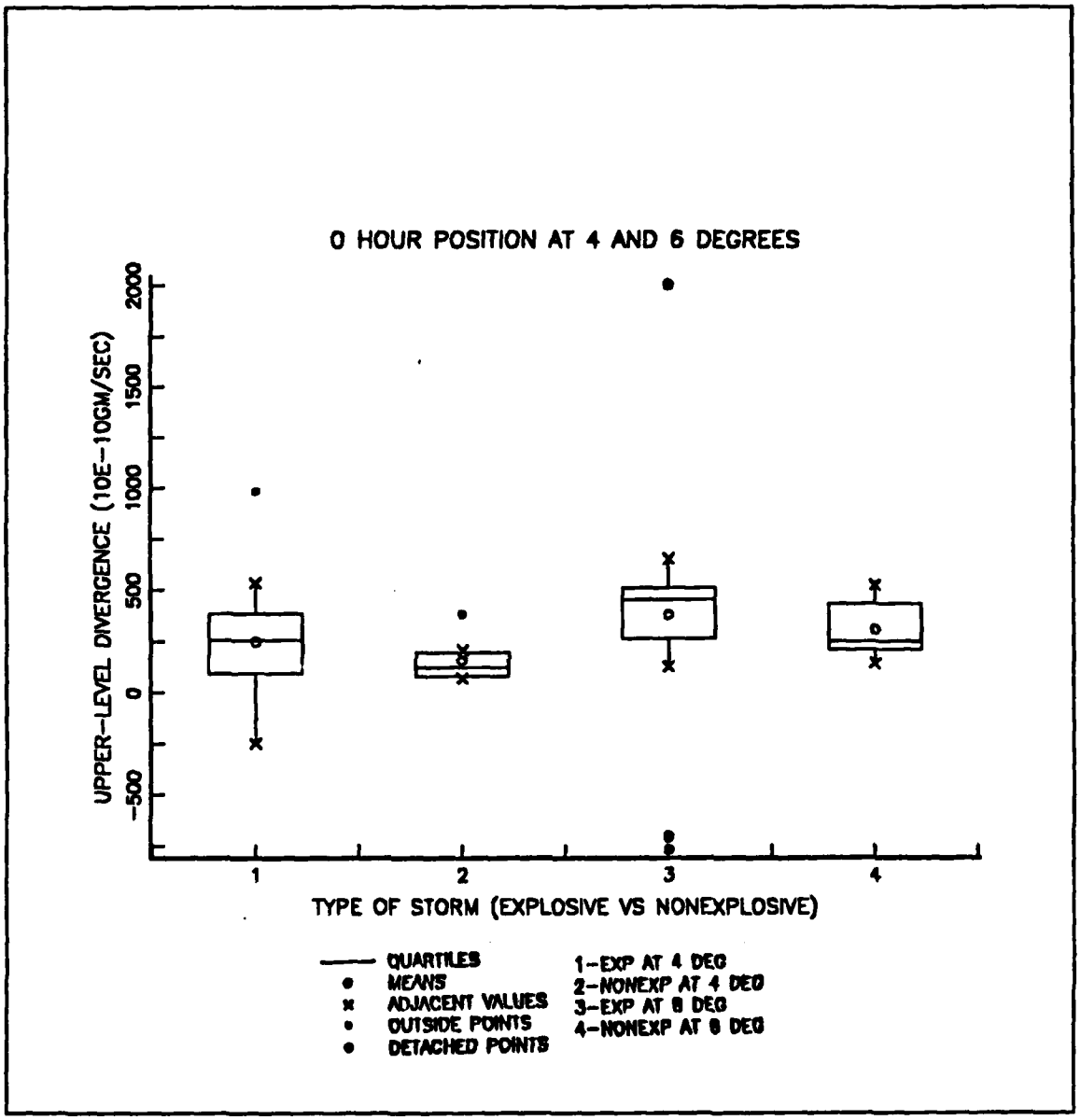

Figure 19. Upper-level divergence, as estimated by the outward mass flux, (500-200 mb) box plots for both storm groups.

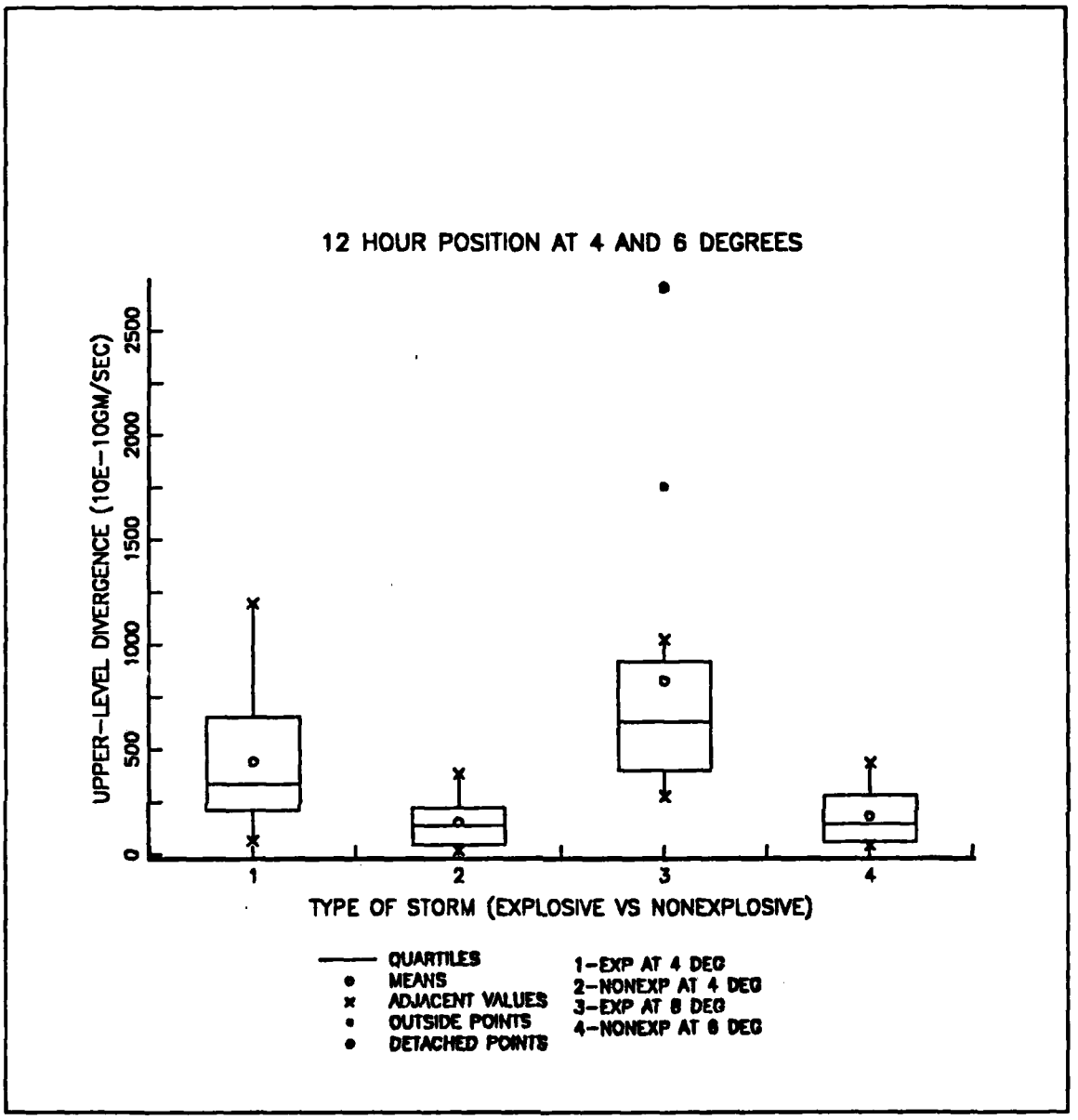

Figure 20. Upper-level divergence, as estimated by the outward mass flux, (500-200 mb) box plots for the 12-h mark.

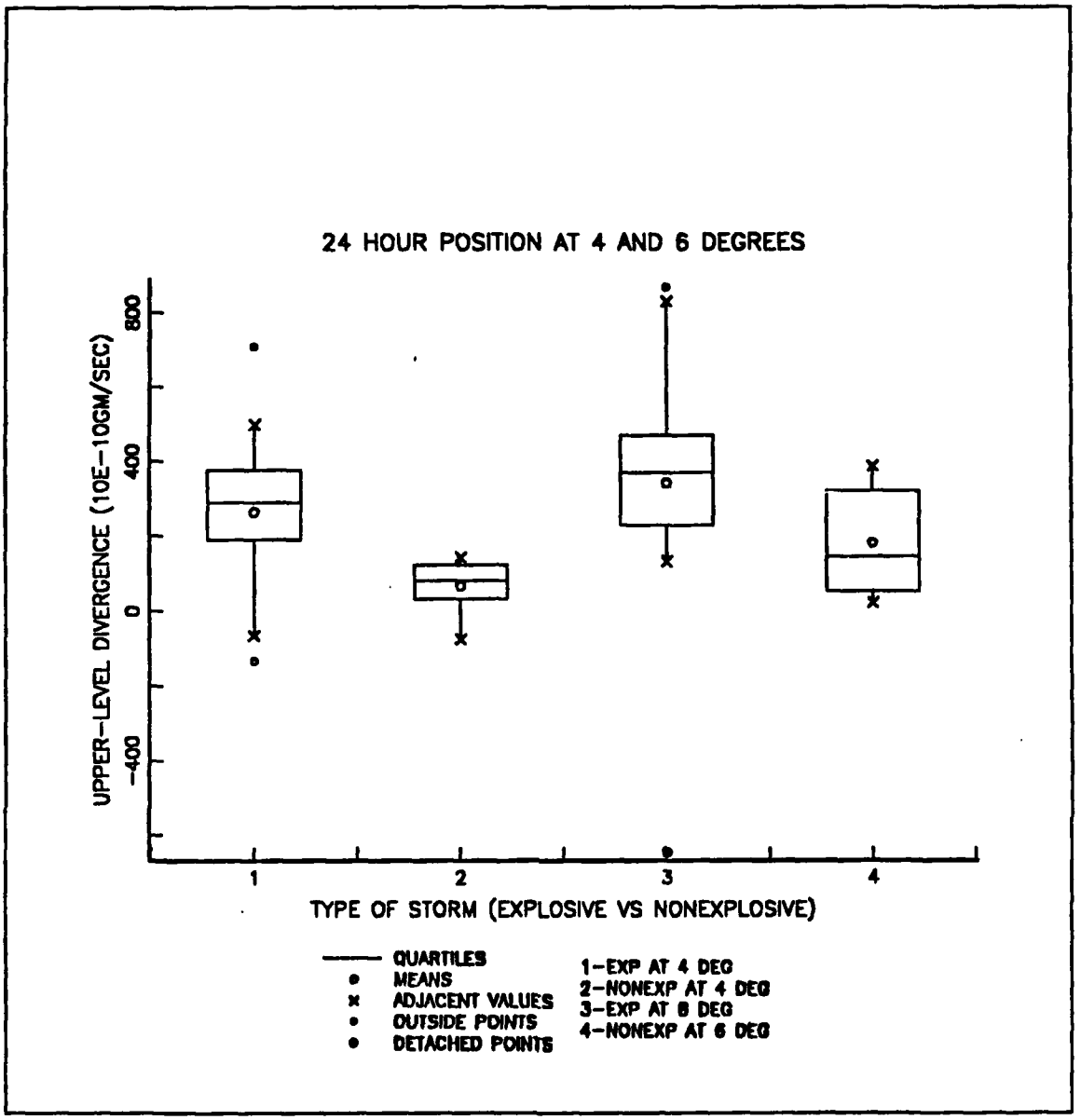

Figure 21. Upper-level divergence, as estimated by the outward mass flux, (500-200 mb) box plots for the 24-h mark.

VII. CONCLUSIONS AND RECOMMENDATIONS

This study of explosive cyclogenesis using the new FGGE data resulted in several conclusions, as follows:

- the upper-level parameters (statistical separation in over half of the terms) were dominant in explosive cyclogenesis, especially during the transition between the incipient and explosive phases.
- the low-level vorticity for the explosive cases displayed a larger growth in magnitude for a 24 h period, in agreement with the sea-level pressure analyses. Even though the nonexplosive cyclones had slightly higher initial values (of low-level absolute vorticity), eventually the explosive storms developed the larger vorticities.
- the low-level baroclinity (as measured from a cross-front temperature difference) had a maximum value at the 12-h mark with slightly larger values for the explosive storms. However, there is no statistical separation in comparing the two storm groups.
- the explosive and nonexplosive storms form in an environment of weak static stability.
- kinematic vertical velocities were more consistent with upper-level physical mechanisms and had less variability than the vertical velocities provided by the ECMWF analyses.
- positioning of the cyclones was critical for obtaining reasonable values for the mass and circulation budgets.
- the new FGGE analyses changed the classification of several explosive and nonexplosive systems and enhanced the overall data set.

The interpretation of the results listed in Chapter Six stem from the vigorous cyclogenesis that was occurring from the onset of the storm to the 12-h point. During this period, the cyclone underwent a self development phase in which the strengthening of the upper-level wave resulted in greater cold advection to the west and greater warm advection to the east. The low-level absolute vorticity continued to grow until the pressure of the cyclone started to rise, which marked end of the cyclogenesis process.

The similarities and differences between the explosive and nonexplosive cyclones remained consistent throughout the rapid development in most cases. The maximum contribution for the upper and lower processes normally occurred at the 12 h mark. For the nonexplosive cases, there was usually a significant decrease after this time. However, the nonexplosive storms did experience higher values for absolute vorticity values than the explosive storms at the initial cyclogenesis. Therefore statistical separation was not

possible for low-level absolute vorticity in the early stages of cyclogenesis. The explosive storms have slightly weaker static stability compared to the nonexplosive ones.

To improve present research efforts the following recommendations are provided:

- more cases of upper-level forcing are necessary to improve the statistical data base for comparison.
- larger sample sizes of cyclones are needed to provide a better Kolmogorov-Smirnov test for goodness of fit for a normal distribution.
- storms should be grouped for only 12 or 24 h of deepening, rather than combined, to maintain consistency of the data set. Given the inherent inaccuracies in central pressure values, a change in pressure divided by the change in time ($\Delta P/\Delta T$) has more signal (less contamination from 'noise') if the total time change (ΔT) is 24 h vice 12 h.
- storms that formed over land and then moved seaward should be excluded from the list. This would preserve the purity of the data set as a study of maritime cyclogenesis.
- more detailed study of upper-tropospheric potential vorticity is necessary to observe upper-level air flow patterns associated with explosive cyclogenesis.
- different quadrants of the cyclone should be investigated for the largest static stability differences.
- more analyses of the moisture variables would be an important addition to the processes being evaluated.

The intensity of the physical mechanisms responsible for explosive cyclogenesis are varied and, even with modern techniques, difficult to consistently forecast. Although the improvement of model skill has occurred due to better analyses, increased resolution and treatment of boundary layer fluxes, initial data input is still the most limiting factor in predictability (Sanders, 1987). Present methods to obtain the necessary data to forecast these mesoscale events are inadequate. Therefore, the mariner must be knowledgeable of the indications for explosive cyclone events while meteorologists continue to pursue this challenge.

APPENDIX A. BASIC EQUATIONS FOR QUASI-LAGRANGIAN BUDGET STUDIES

1. Definition of Budget Integrated Property (F)

$$F = \int_{V_\eta} \rho J_\eta f r^2 \sin\beta dV_\eta \tag{1}$$

where:

F - is the total property.

V_η - volume of cylinder represented in coordinate system η ,α,and β.

ρ - density.

$|J_\eta|$ - Jacobian transformation from η to z coordinate system.

f - any specific property.

r - radius in the horizontal.

β- angle between the local vertical and the edge of the storm measured at the center of the earth.

2. Mass Budget Equation

$$\frac{dM}{dt} = \mathrm{LT} + VT \tag{2}$$

where:

LT - is the lateral transport of the mass of F.

VT - is the vertical transport of the mass of F.

3. Lateral Transport (in detail)

$$LT = -\int_{\eta_b}^{\eta_t}\int_{0}^{2\pi} \rho J_\eta (u - w)_\beta fr \sin\beta d\alpha d\eta \mid_{\beta_B} \tag{3}$$

where:

η_t - is the top coordinate.

η_B - is the bottom coordinate.

u - relative wind vector in the radial direction.

w - storm motion vector in the radial direction.

4. Vertical Transport (in detail)

$$VT = -\int_{0}^{B}\int_{0}^{2\pi} \rho J_\eta \left(\frac{d\eta}{dt} - \frac{d\eta_B}{dt}\right) fr^2 \sin\beta d\alpha d\beta \mid_\eta \tag{4}$$

where:

$\frac{d\eta}{dt}$ - is the change in the η coordinate system with respect to time.

$\frac{d\eta_B}{dt}$ - the change in the top and bottom boundary of the η coordinate system with respect to time.

5. Vorticity Budget Equation

The vorticity budget equation shows the contributions to vorticity changes from the lateral and vertical fluxes (transports) as sources sinks. The following equation describes these terms:

$$\frac{\partial C_a}{\partial t} = LT(\zeta_a) + DVT(\zeta_a) + S(\zeta_a) \tag{5}$$

where:

C_a - is the absolute circulation.

ζ_a - is the absolute vorticity.

$LT(\zeta_a)$ - is the lateral transport of absolute vorticity that includes the mean and eddy modes, as well as the horizontal divergence and advection.

$DVT(\zeta_a)$ - is the vertical transport of absolute vorticity that includes vertical divergence and advection.

$S(\zeta_a)$ - is the sink of absolute vorticity through the divergence, tilting and frictional dissipation terms.

The source or sink terms originate from the generation or dissipation of vorticity within the budget volume, and in isobaric coordinates represent the divergence, tilting and frictional terms. To gain a better physical understanding of the vorticity budget equation, the absolute circulation is written in terms of Stokes' line integral theorem:

$$C_a = \int_L \zeta_a \vec{u} \cdot \vec{n}\, dl = \int_A \int \nabla \cdot \zeta_a \vec{u}\, dA \tag{6}$$

The total flux $\vec{u}\zeta_a$ can be divided into the divergent and advective components as follows:

$$\nabla \cdot \zeta_a \vec{u} = \zeta_a (\nabla \cdot \vec{u}) + \vec{u} \cdot \nabla \zeta_a \tag{7}$$

where the terms on the right side of the equation are defined as:

$\zeta_a(\nabla \cdot \vec{u})$ - vorticity divergence.

$\vec{u} \cdot \nabla \zeta_a$ - vorticity advection component.

APPENDIX B. STATISTICAL ANALYSIS FOR NORMAL DISTRIBUTION

The statistical analysis for normal distribution on the FGGE cyclone diagnostic terms was accomplished using the Kolmogorov-Smirnov test for goodness of fit (Lilliefors, 1967). For a sample size n, an empirical distribution function $F_n(x)$ is defined as follows:

$$F_n(x) = k/n \tag{8}$$

where:

$F_n(x)$ - is the empirical distribution function for $x_{(i)} \leq x \leq x_{(i-1)}$.

k - is the number of observations not greater than x.

$x_{(1)}$ to x_n - denotes the sample values.

In this test, the null hypothesis was that the sample had been drawn from a normal distribution $F_n(x)$, which should be close to F(x). The Kolmogorov-Smirnov test statistic D was based on the maximum difference between the observed and hypothesized cumulative distribution functions as follows:

$$D = \max |F_n(x) - F(x)| \tag{9}$$

Comparison of the critical values of D for a two-tailed test was conducted under the null hypothesis at a significance level equal to 0.10. The null hypothesis was rejected if D exceeded the critical value. This test assumed that the observed distribution was unknown and continuous, and that x_1 through x_n did not directly depend on the choice of the distribution (Conover, 1980).

Examples of the graphical representations of the data distributions are shown in Figs. 22 through 27. The data for the upper-level divergence (at the 4° latitude radius and T = 0 h) of an explosive storm group are displayed in the first three figures , and for the nonexplosive case in the latter three diagrams. The histograms in Figs. 22 and 25 illustrate the relative frequency distribution for the 13 explosive and eight nonexplosive storms with a normal distribution curve for comparison. Figs. 23 and 26 show the normal cumulative distribution function, where the smooth curve represents the continuous area under the normal distribution curve. The Kolmogorov-Smirnov boundaries

are the two diametrically opposed dotted lines and the middle line represents the observed data. The probability plots (Figs. 23 and 27) demonstrate the same normal distribution using a vertical percentile scale. This scale has been modified in the vertical to allow an easier visual comparison of the normal distribution (the straight line) to the observed data.

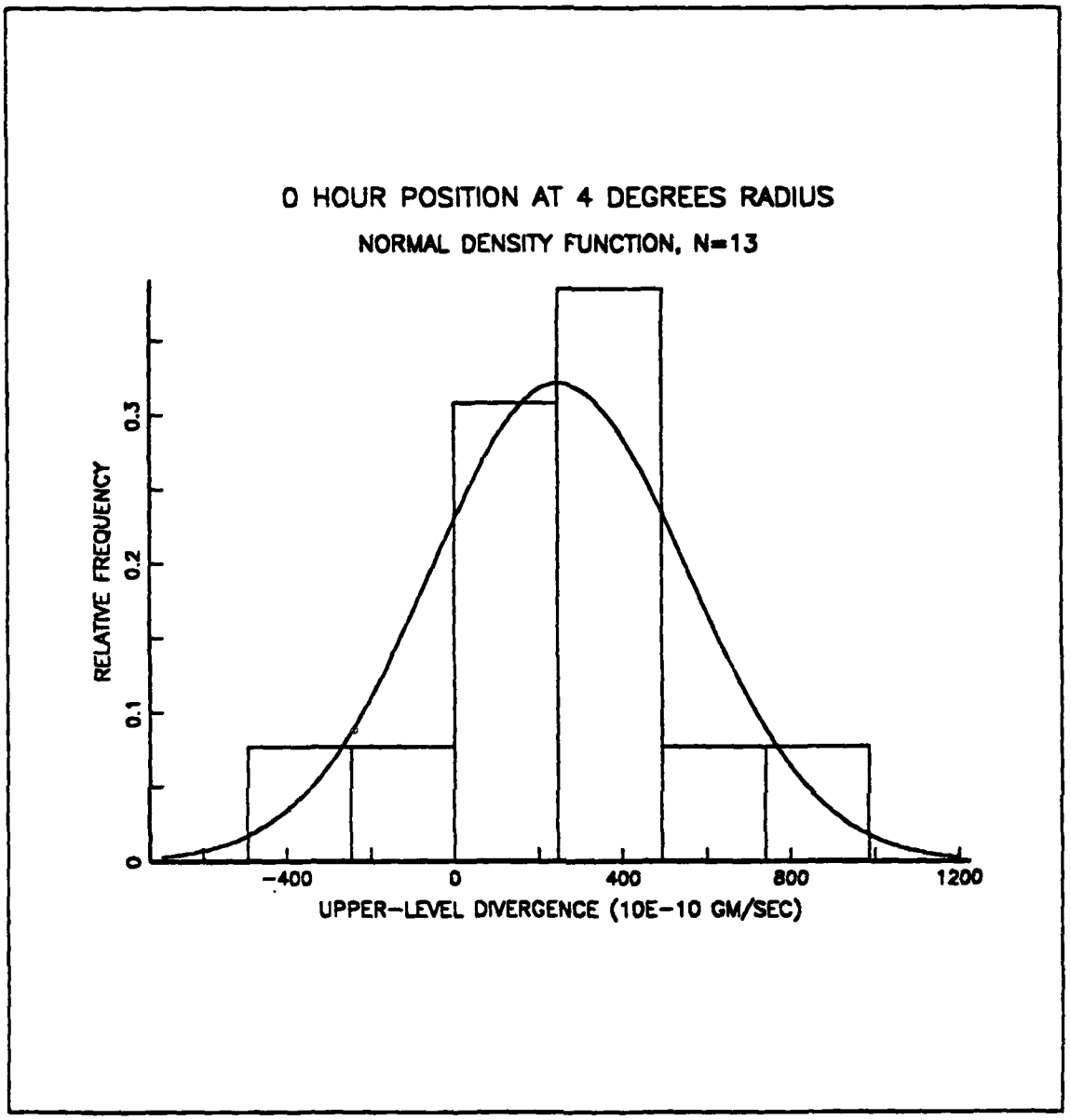

Figure 22. Histogram distribution for upper-level divergence for an explosive storm group.

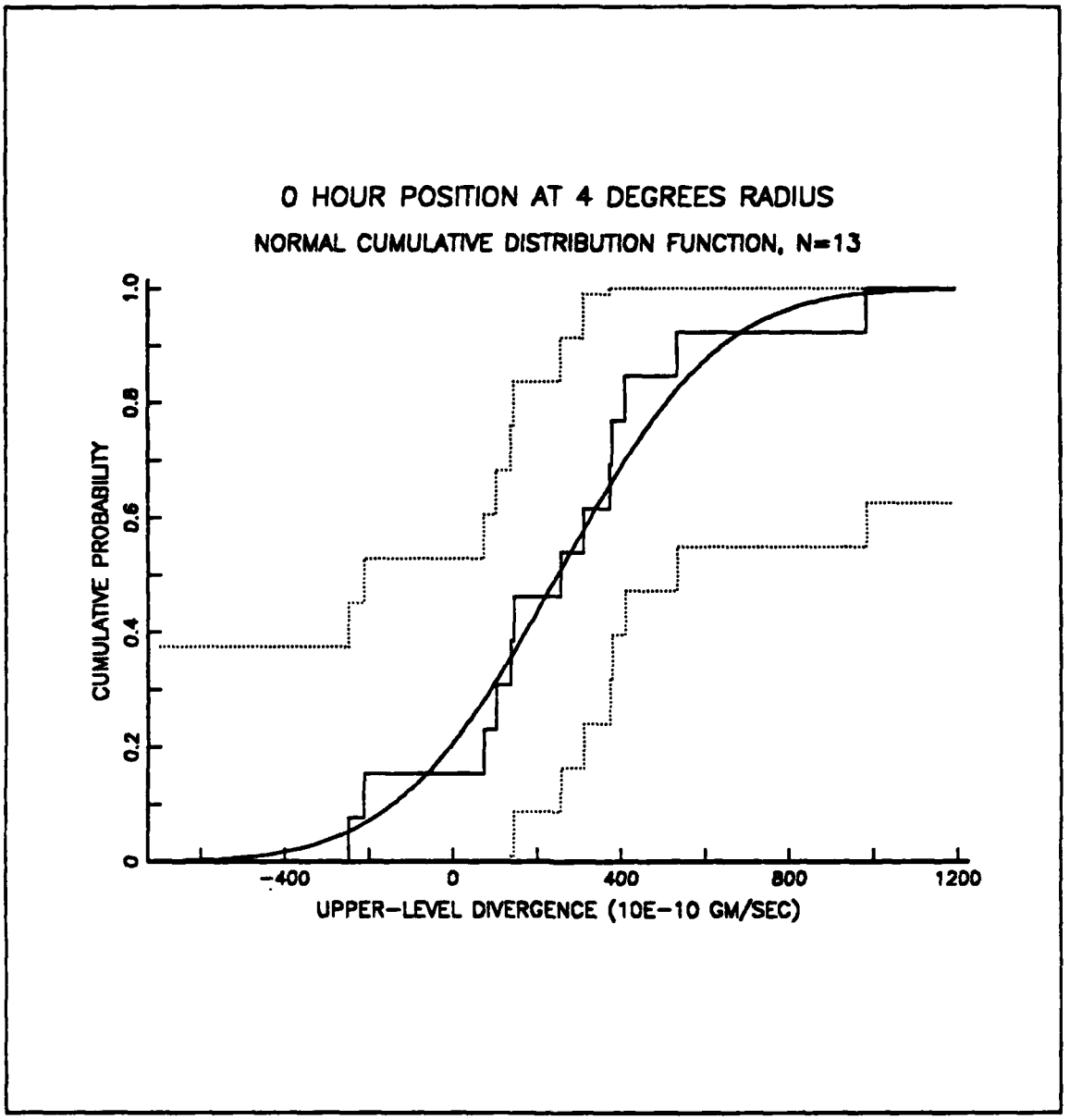

Figure 23. Normal cumulative distribution curve for an explosive storm group.

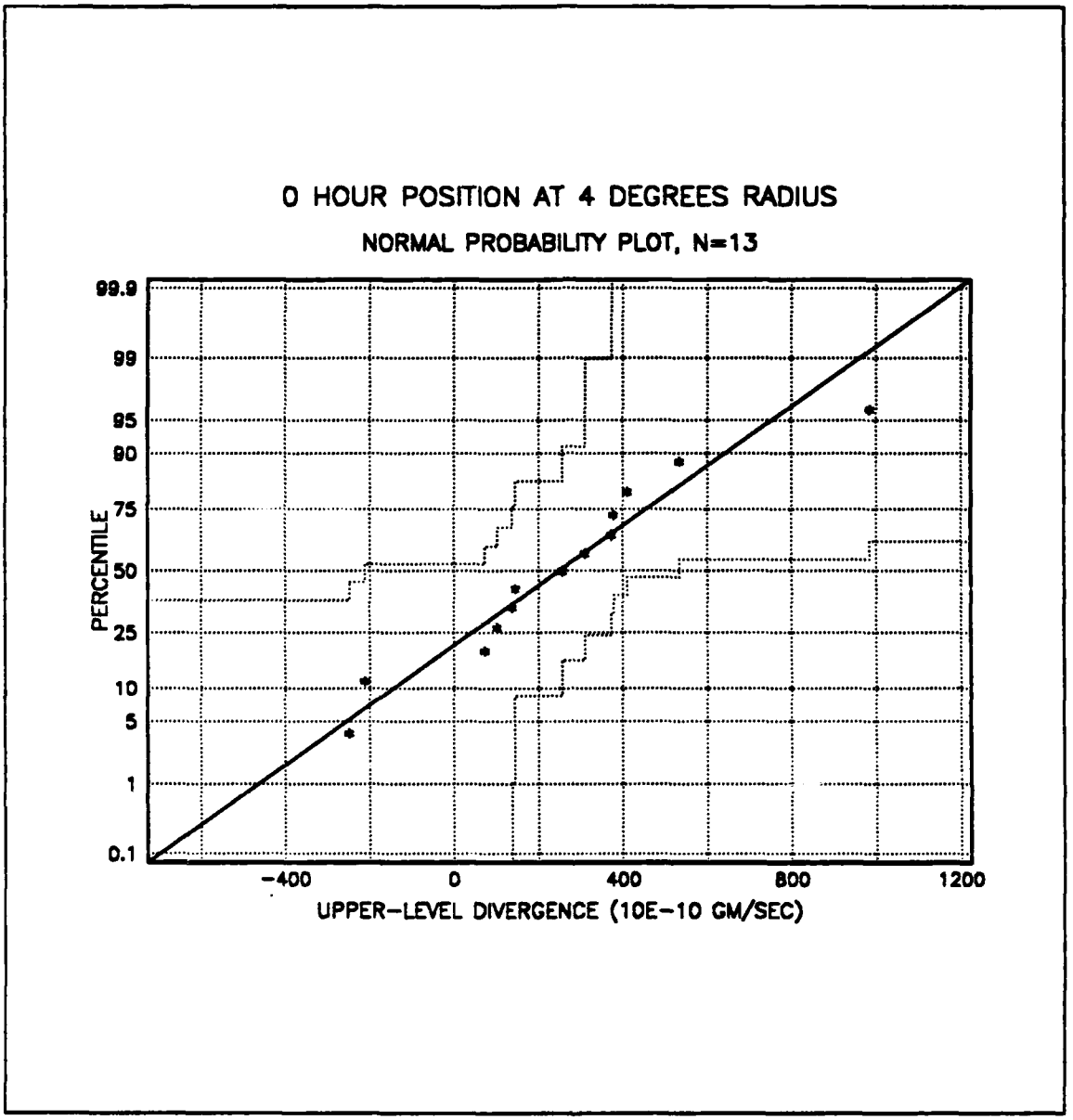

Figure 24. Probability plot for an explosive storm group.

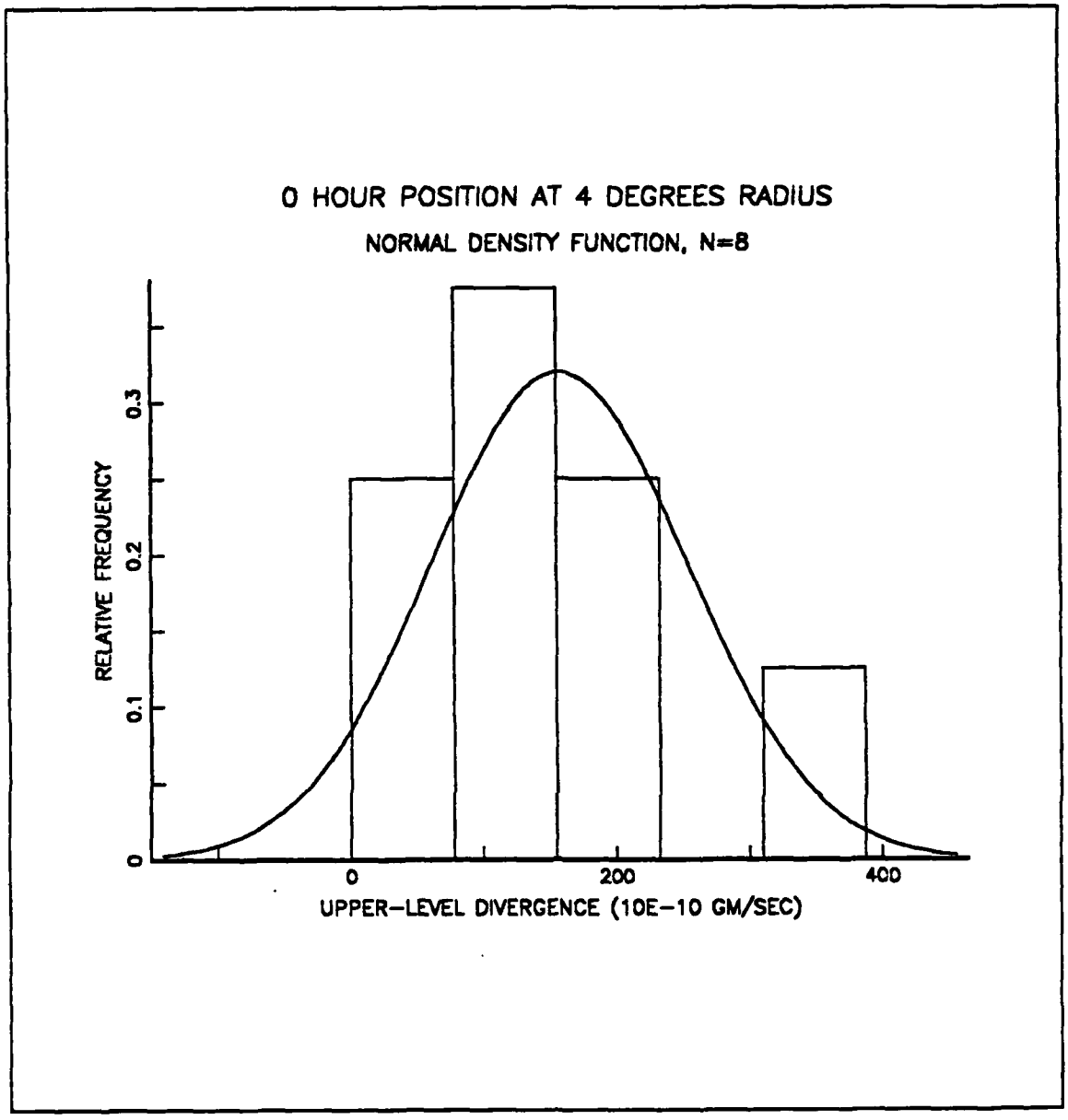

Figure 25. Histogram distribution for upper-level divergence for a nonexplosive storm group.

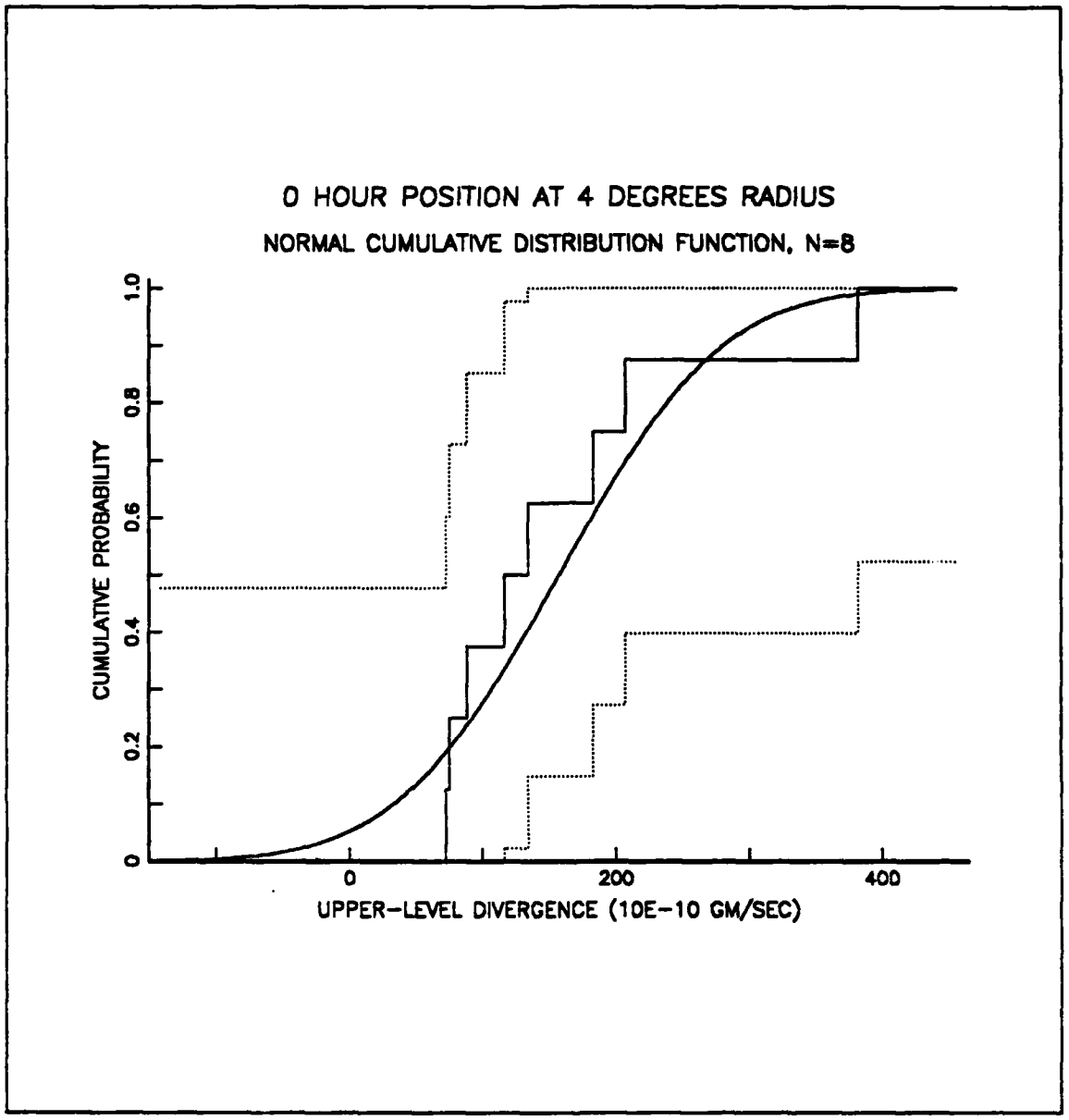

Figure 26. Cumulative distribution curve for a nonexplosive storm group.

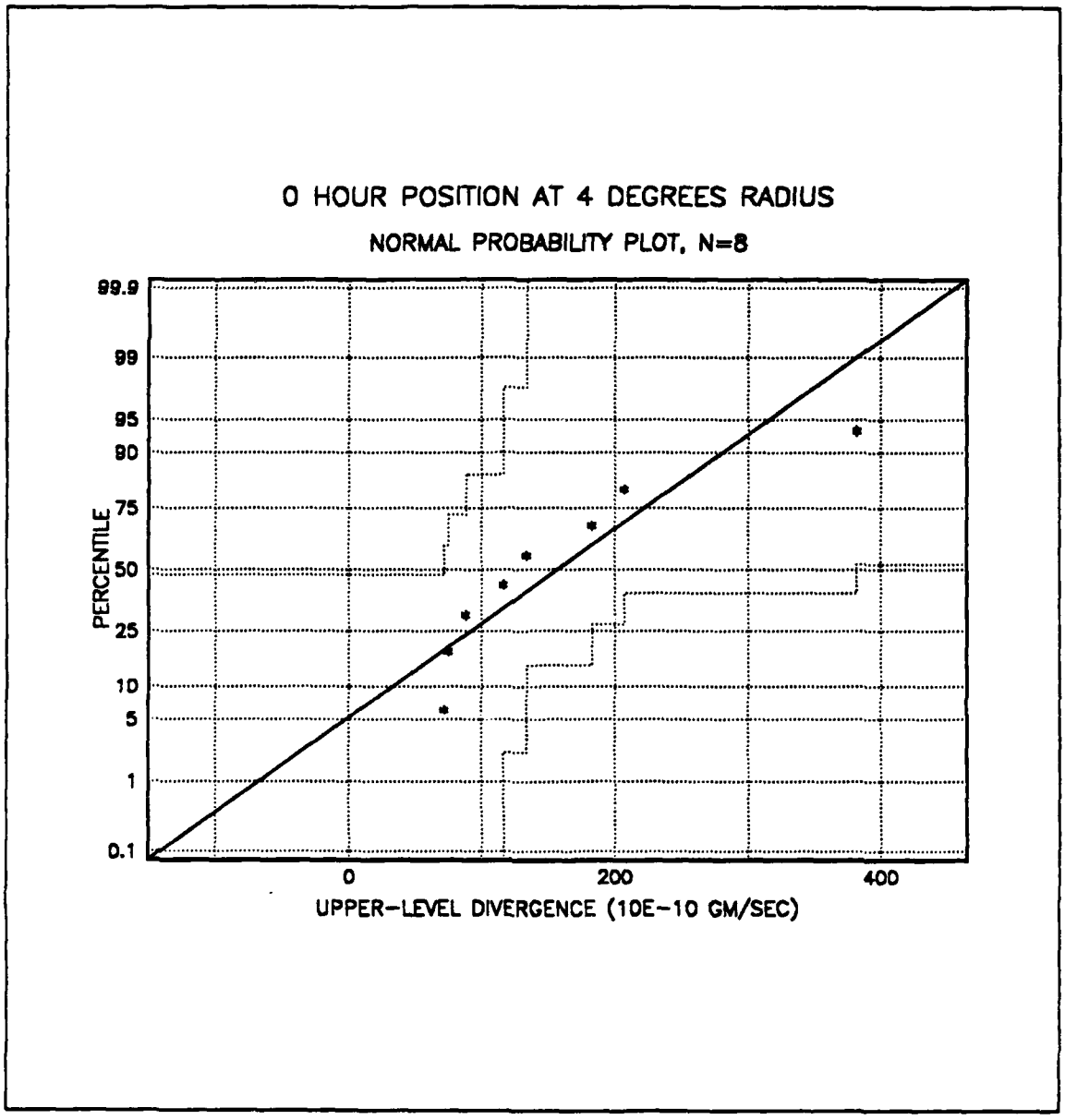

Figure 27. Probability plot for a nonexplosive storm group.

LIST OF REFERENCES

Anthes, R. A., Y. H. Kuo and J. R. Gyakum, 1983: Numerical simulation of a case of explosive maritime cyclogenesis. *Mon. Wea. Rev.*, **100**, 1174-1188.

Bengtssen, L., M. Kanamitsu, P. Kallberg and S. Uppala, 1982: FGGE 4-dimensional data assimilation at ECMWF. *Bull. Amer. Meteor. Soc.*, **63**, 29-43.

Bjorheim, K., P. Julian, M. Kanamitsu, P. Kallberg, P. Price, S. Tracton and S. Uppala, 1981: FGGE III-B daily global analyses - 4 Parts. European Centre for Medium-range Weather Forecasts., Reading, U.K.

Bosart, L. F., 1981: The Presidents' Day snowstorm of 18-19 February 1979; A subsynoptic scale event. *Mon. Wea. Rev.*, **109**, 1542-1566.

Bosart, L. F., and S. C. Lin, 1984: A diagnostic analysis of the Presidents' Day storm of February 1979. *Mon. Wea. Rev.*, **112**, 2148-2177.

Calland, W. E., 1983: Quasi-Lagrangian diagnostics applied to an extratropical explosive cyclogenesis in the North Pacific. M.S. Thesis, Naval Postgraduate School, Monterey, CA, 154 pp.

Chambers J. M., W. S. Cleveland, B. Kleiner, and P. A. Tukey, 1983: Graphical methods for data analysis., Duxbury Press, Boston, MA, 395 pp.

Conover, W. J., 1980: Practical nonparametric statistics. 2nd ed., Wiley & Sons, New York, 462 pp.

Devore, J. L., 1987: Probability and statistics for engineering and the sciences. 2nd ed., Brooks Cole Pub. Co., Monterey, CA, 662 pp.

Emanuel, K. A., 1983: On assessing local conditional symmetric instability from atmospheric soundings. *Mon. Wea. Rev.*, **111**, 2016-2033.

Gyakum, J. R., 1983a: On the evolution of the QE-II storm. Part I: synoptic aspects. *Mon. Wea. Rev.*, **111**, 1137-1155.

Gyakum, J. R., 1983b: On the evolution of the QE-II storm. Part II: dynamic and thermodynamic structure. *Mon. Wea. Rev.*, **111**, 1156-1173.

Halem, M., E. Kalnay, W. E. Baker and R. Atlas, 1982: An assessment of the FGGE satellite observing system during SOP-I. *Bull. Amer. Meteor. Soc.*, **63**, 407-427.

Johnson, D.R., and W. K. Downey, 1975a: Azimuthally averaged transport and budget equations for storms: quasi-Lagrangian diagnostics. *Mon. Wea. Rev.*, **103**, 967-979.

Johnson, D.R., and W. K. Downey, 1975b: The absolute angular momentum of storms: quasi-Lagrangian diagnostics. *Mon. Wea. Rev.*, **103**, 1063-1076.

Lilliefors, H. W., 1967: On the Kolmogorov-Smirnov test for normality with mean and variance unknown. *Journal of American Statistical Association*, **62**, 387-389.

O'Brien, J. J., 1970: Alternative solutions to the classical vertical velocity problem. *J. Appl. Meteor.*, **2**, 197-203.

Paegle, J., 1986: Summary of the national conference on the scientific results of the first GARP global experiment, January 14-17, 1986. *Bull. Amer. Meteor. Soc.*, **67**, 1487-1492.

Pagnotti, V., and L. F. Bosart, 1984: Comparative diagnostic case study of east coast secondary cyclogenesis under weak versus strong synoptic-scale forcing. *Mon. Wea. Rev.*, **112**, 5-30.

Petterssen, S., 1956: Weather analysis and forecasting, Vol. 1, Motion and Motion Systems. McGraw-Hill Book Co. Inc., 428 pp.

Rogers, E., and L. F. Bosart, 1986: An investigation of explosive deepening oceanic cyclones. *Mon. Wea. Rev.*, **114**, 702-718.

Sanders, F., 1987: Skill of NMC operational dynamical models in prediction of explosive cyclogenesis. *Weather and Forecasting*, **2**, 322-336.

Sanders, F., and J. R. Gyakum, 1980: Synoptic-dynamic climatology of the "bomb". *Mon. Wea. Rev.*, **108**, 1589-1606.

Shaw, D. B., P. Lonnberg, A. Hollingsworth and P. Unden, 1987: Data assimilation. The 1984 85 revisions of the ECMWF mass and wind analysis. *Quart. J. Roy. Meteorol. Soc.*, **113**, 533-566.

Smith, D. H., 1986: A diagnostic investigation of explosive maritime cyclogenesis during FGGE. M.S. Thesis, Naval Postgraduate School, Monterey, CA, 53 pp.

Uccellini, L. W., 1984: Comments on comparative diagnostic case study of east coast secondary cyclogenesis under weak versus strong synoptic scale forcing. *Mon. Wea. Rev.*, **112**, 2540-2543.

Uccellini, L. W., P. J. Kocin, R. A. Peterson, C. H. Wash and K. F. Brill, 1984: The Presidents' Day cyclone of 18-19 February 1979: synoptic overview and analysis of the subtropical jet streak influencing the precyclogenetic period. *Mon. Wea. Rev.*, **112**, 31-55.

Uccellini, L. W., D. Keyser, K. F. Brill and C. H. Wash, 1985: The Presidents' Day cyclone of 18-19 February 1979: amplification and associated tropopause folding on rapid cyclogenesis. *Mon. Wea. Rev.*, **113**, 962-988.

Uccellini, L. W., 1986: The possible influence of upstream upper-level baroclinic processes on the development of the QE II storm. *Mon. Wea. Rev.*, **114**, 1019-1027.

Uppala, S., 1986: The assimilation of the final FGGE data set set at ECMWF. Part I. *Proceedings of U.S. national conference on the scientific results of the first GARP*

global experiment. FGGE, 14-17 January 1986, American Meteorological Society, 24-30.

Wash, C. H., 1978: Diagnostics of observed and numerically simulated extratropical cyclones. PhD. Thesis, Department of Meteorology, University of Wisconsin, Madison, WI, 215 pp.

Wash, C. H., J. E. Peak, W. E. Calland and W. A. Cook, 1988: Diagnostic study of explosive cyclogenesis during FGGE. *Mon. Wea. Rev.*, **116**, 431-451.

INITIAL DISTRIBUTION LIST

		No. Copies
1.	Defense Technical Information Center Cameron Station Alexandria, VA 22304-6145	2
2.	Library, Code 0142 Naval Postgraduate School Monterey, CA 93943-5002	2
3.	Chairman (Code 63Rd) Department of Meteorology Naval Postgraduate School Monterey, CA 93943-5000	1
4.	Chairman (Code 68Co) Department of Oceanography Naval Postgraduate School Monterey, CA 93943-5000	1
5.	Professor Carlyle H. Wash (Code 63Wx) Department of Meteorology Naval Postgraduate School Monterey, CA 93943-5000	9
6.	Professor Russell L. Elsberry (Code 63Es) Department of Meteorology Naval Postgraduate School Monterey, CA 93943-5000	1
7.	LCDR Eric J. Wright, USN 110 Mervine St Monterey, CA 93943-5000	4
8.	Professor Dave A. Schrady (Code 55Sd) Department of Operations Research Naval Postgraduate School Monterey, CA 93943-5000	1
9.	Professor Donald A. Danielson (Code 53Dd) Department of Mathematics Naval Postgraduate School Monterey, CA 93943-5000	1

10. Director Naval Oceanography Division — 1
Naval Observatory
34th and Massachusetts Avenue NW
Washington, DC 20390

11. Commander Naval Oceanography Command — 1
Naval Oceanography Command
Stennis Space Center
Bay St. Louis, MS 39522

12. Commanding Officer — 1
Naval Oceanographic Office
Stennis Space Center
Bay St. Louis, MS 39522

13. Commanding Officer — 1
Fleet Numerical Oceanography Center
Monterey, CA 93943

14. Commanding Officer — 1
Naval Environmental Prediction Research Facility
Monterey, CA 93943

15. Chairman, Oceanography Department — 1
U. S. Naval Academy
Annapolis, MD 21402

16. Chief of Naval Research — 1
800 North Quincy Street
Arlington, VA 22217

17. Office of Naval Research (Code 420) — 1
Naval Ocean Research and Development Activity
800 North Quincy Street
Arlington, VA 22217